Dual-acting antitumor Pt(IV) prodrugs of kiteplatin with dichloroacetate axial ligands.

Salvatore Savino,[1] Valentina Gandin,[2] James D. Hoeschele,[3] Cristina Marzano,[2] Giovanni Natile,[1,] Nicola Margiotta.[1,*]*

[1]Dipartimento di Chimica, Università degli Studi di Bari Aldo Moro, via E. Orabona, 4, 70125 Bari (Italy);

[2]Dipartimento di Scienze del Farmaco, Università di Padova, via Marzolo 5, 35131 Padova (Italy);

[3]Department of Chemistry, Eastern Michigan University, Ypsilanti, MI, USA 48197.

***Corresponding Authors:** NM, Tel. +39-080-5442759; e-mail: nicola.margiotta@uniba.it. GN, Tel. +39-080-5442774; email: giovanni.natile@uniba.it.

Abstract

With the aim to obtain dual acting drugs able to target both nuclear DNA and mitochondria, Pt(IV) Kiteplatin derivatives having dichloroacetate (DCA) ligands in axial positions have been synthesized. The rather fast hydrolysis ($t_{1/2}$ of ca. 1h) and reduction (by ascorbic acid) of these Pt(IV) derivatives did not impede a potent pharmacological effect on tumor cells. Moreover, similarly to kiteplatin, also the Pt(IV)-DCA compounds proved to be capable of overcoming oxaliplatin-resistance, which is particularly important in view of the fact that metastatic colorectal cancer is the third most common cancer in males and the second in females. The possible role of DCA released by the Pt(IV) compounds in eliciting the antiproliferative activity has also been investigated. Pt(IV)-DCA compounds determine a substantial increase of ROS production, blockage

of oxidative phosphorylation, hypopolarization of the mitochondrial membrane, and caspase-3/7 mediated apoptotic cell death.

Introduction.

Platinum(II) coordination compounds are well-known antiproliferative agents.[1] Among these, cisplatin, carboplatin and oxaliplatin (Figure 1) have received Food and Drug Administration approval and are used in the clinic worldwide.[2,3] Although previous studies have identified differences in cellular response between cisplatin and oxaliplatin, only recently Lippard and Hemann highlighted that the different spectrum of activity between cisplatin and oxaliplatin is consistent with the ability of the latter to mainly inhibit rRNA synthesis rather than DNA synthesis, and to consequently induce ribosome biogenesis stress.[4] However, there are some limitations to the use of these drugs, such as the appearance of resistance and induction of severe side effects.[5] Moreover, cisplatin and oxaliplatin require hospitalization for intravenous administration, which is associated with a poor patient compliance. To overcome at least some of these drawbacks, new platinum drugs, based on the platinum(IV) core, have been developed. That platinum(IV) complexes, such as *cis*-$[PtCl_4(NH_3)_2]$, could have anticancer activity was already known from the time of Rosenberg's discovery of cisplatin.[6] The potential advantages of platinum(IV) complexes (Figure 2) rely on their ability to act as pro-drugs.[7] They are stable in the blood stream, so reducing the incidence of undesired toxic side effects, and, being kinetically inert, allow for oral administration.[8] Once entered the cell, Pt(IV) compounds undergo reduction, with release of the axial ligands and of the active Pt(II) species.[9] The latter can then undergo hydrolysis and give electrophilic attack on target DNA. Axial ligands can also be used to tune the lipophilicity of the Pt(IV) prodrugs (for a better uptake from tumor cells) and their redox properties, both factors being relevant to the anticancer efficacy.[10,11,12] The first two Pt(IV) compounds that underwent phase I clinical trials, tetraplatin (tetrachlorido-*R*,*R*-1,2-diaminocyclohexaneplatinum(IV)) and iproplatin

(*cis*-dichlorido-*trans*-dihydroxido-bis-isopropylamine-platinum(IV)), showed unfavorable pharmacokinetic behaviors because of their too high or too low reduction potential (–90 and –730 mV for tetraplatin and iproplatin, respectively). An intermediate behavior was observed for Pt(IV) complexes with axial carboxylato ligands.[13,14] For instance, satraplatin (*cis*-dichlorido-*trans*-diacetato-*cis*-ammine-cyclohexylamine-platinum(IV)) has a reduction potential of –250 mV and was the first platinum complex reported to have oral activity. Satraplatin underwent Phase III clinical trials (Satraplatin and Prednisone Against Refractory Cancer - SPARC, NCT00069745) but, despite the positive outcome, the successive claim for FDA approval was rejected.[15]

In addition, octahedral Pt(IV) complexes offer the opportunity to design dual-acting Pt drugs if the axial ligands, released upon reduction, are endowed with own pharmacological activity.[16,17,18] In this context, Pt(IV) complexes with "antimitochondrial" ligands in the axial positions, such as mitaplatin (*cis,trans,cis*-$[PtCl_2(DCA)_2(NH_3)_2]$, DCA = HCl_2CCOO^-, dichloroacetate; Figure 2), have recently been investigated.[19]

A peculiar feature of cancer cells is to produce most of their energy by glycolysis rather than by mitochondrial oxidative metabolism. This phenomenon, known as the "Warburg effect" and first described by Otto Warburg over 80 years ago, has been reinterpreted over the last decades in the light of the increasing recognition of the central role of mitochondria in cancer.[20] There is evidence that disturbances in mitochondrial metabolic pathways correlate with tumorigenesis and provide a rationale for the exploitation of mitochondria as targets for anti-cancer therapy.[21] In the specific case of mitaplatin, after reduction inside the cancer cell, two molecules of DCA are released in addition to active cisplatin. Dichloroacetate (DCA), an off-patent drug structurally analogous to pyruvate, can inhibit the pyruvate dehydrogenase kinase (PDK); this leads to the reactivation of the pyruvate dehydrogenase complex, which directs a greater flux of pyruvate into the mitochondria and promotes glucose oxidation over glycolysis. Ultimately, DCA-mediated PDK inhibition activates the mitochondrial apoptosis in cancer cells and inhibits tumor growth.[22] Although to date

there are no published reports on DCA analogs administered to humans, the discovery of DCA as a potential anticancer agent has renewed the interest in developing association compounds between DCA and other antitumor drugs.[23,24]

Obviously, in addition to the axial ligands, also the equatorial ligands contribute to the cytotoxicity of Pt(IV) pro-drugs. Indeed, the equatorial ligands determine the nature of the Pt(II) active species released after intracellular reduction. In this context it is worth mentioning the Pt(II) derivative [$PtCl_2$(*cis*-1,4-DACH)] (**1**, DACH = diaminocyclohexane), also named kiteplatin (Figure 1), which has recently proved to be endowed with very promising anticancer activity. Kiteplatin contains an isomeric form of the diamine ligand (1*R*,2*R*-DACH) present in oxaliplatin[25] and is active against cisplatin-resistant (ovarian C13*) and oxaliplatin-resistant (colon LoVo-OXP) cell lines, suggesting that the spectrum of activity of kiteplatin could be different from those of cisplatin and oxaliplatin. Moreover, tested *in vivo* against the murine Lewis lung carcinoma, kiteplatin was found to possess an efficacy similar to that of cisplatin and to be better tolerated than the reference metallo-drug.[25] Furthermore, it has been established that the 1,2-GG intrastrand crosslinks formed by kiteplatin are removed by DNA repair systems with lower efficiency than those formed by cisplatin and are more effective in inhibiting DNA polymerases such as the model prokaryotic DNA polymerase I (KF^-) of the A-family and the eukaryotic translesion DNA polymerase η (Polη) of the Y-family human DNA polymerases.[26,27]

In the present investigation, we have focused on Pt(IV) complexes derived from kiteplatin (**1**) and its oxalate analogue [Pt(OXA)(*cis*-1,4-DACH)] (**4**) by addition of two DCA ligands in axial positions; the major aim being the obtainment of dual acting complexes able to target both nuclear DNA and mitochondria. The newly synthesized Pt(IV) complexes, *cis,trans,cis*-[$PtCl_2(DCA)_2$(*cis*-1,4-DACH)] (**3**) and *cis,trans,cis*-[Pt(OXA)$(DCA)_2$(*cis*-1,4-DACH)] (**6**), have been characterized by spectroscopic techniques and the stability to hydrolysis of **3** at pH = 7.4 and 37 °C has been monitored by ^{1}H-NMR. Moreover, the reduction of compound **3** and of the parent complex

cis,trans,cis-[$PtCl_2(OH)_2$(*cis*-1,4-DACH)] (**2**) by the biologically relevant reductant ascorbic acid has also been investigated.

All the Pt(IV) compounds were tested *in vitro* against a series of different tumor cell lines, some of which were selected for their resistance to cisplatin and oxaliplatin. Cellular accumulation and DNA platination levels, as well as mitochondrial functionality, were analyzed in an attempt to gain insights into the mechanism of action of these dual-acting pro-drugs. Finally, as a further step, the antitumor activity of **3** was assessed *in vivo* in a solid syngeneic murine model (the Lewis Lung Carcinoma).

Results and discussion

Synthesis and characterization of the compounds.

For the preparation of the Pt(IV) derivatives, kiteplatin, [$PtCl_2$(*cis*-1,4-DACH)] (**1**), and its congener with different leaving group, [Pt(OXA)(*cis*-1,4-DACH)] (**4**), were first oxidized with hydrogen peroxide in water (Scheme 1) to yield *cis,trans,cis*-[$PtCl_2(OH)_2$(*cis*-1,4-DACH)] (**2**)[28] and *cis,trans,cis*-[Pt(OXA)$(OH)_2$(*cis*-1,4-DACH)] (**5**), respectively, and then treated with an excess of dichloroacetic anhydride.[16,29]

We have previously shown that the intermediate Pt(IV) species **2** is not stable in solvents such as DMSO and DMF where it undergoes a heat- or photo-assisted reduction with back formation of kiteplatin.[30] Hence, the condensation reaction with dichloroacetic anhydride was performed in the dark at room temperature.

The compounds were characterized by elemental analysis, ESI-MS, and NMR (see Supporting Information). The ^{1}H NMR of compound **3** in DMSO-d_6 is shown in Figure 3. The singlet, with Pt satellites, located at 7.92 ppm ($^2J_{Pt\text{-}H}$= 58.5 Hz) and assigned to the aminic protons of coordinated *cis*-1,4-DACH is located at lower field with respect to the corresponding signal in compound **2** (6.33 ppm). The deshielding is probably due to the presence of the carboxylic groups of coordinated

DCA in axial positions (hydrogen bond formation between axial C=O and coordinated NH_2 has been observed in similar systems).[31] The singlet located at 6.58 ppm and assigned to the methynic proton of coordinated dichloroacetate is similar to that found in the analogous complex *cis*,*trans*,*cis*-[Pt(OXA)(DCA)$_2$(1*R*,2*R*-DACH)] (6.55 ppm).[32] The methynic and methylenic protons of coordinated DACH give a singlet, with Pt satellites ($^3J_{Pt-H}$= 74.04 Hz), at 3.03 ppm and a multiplet integrating for eight protons at 1.63 ppm, respectively.

The [^{1}H-^{195}Pt]-HSQC 2D NMR spectrum of compound **3** (also shown in Figure 3) exhibits two cross peaks located at 7.92/1196.30 and 3.03/1196.30 ppm (^{1}H/^{195}Pt). The ^{195}Pt chemical shift is at lower field with respect to that of the precursor compound **2** (964.6 ppm in DMSO-d_6) but is in good agreement with that reported for similar Pt(IV) dicarboxylato derivatives and for mitaplatin (1205.28 ppm in DMSO-d_6).[14,16,19,28]

The [^{1}H-^{13}C]-HSQC 2D NMR spectrum (data not shown) shows one cross peak appearing at 6.58/65.40 ppm (^{1}H/^{13}C) belonging to the methynic group of coordinated dichloroacetate (^{13}C chemical shift of 65.27 ppm in mitaplatin)[19] and two cross peaks located at 3.03/50.10 and 1.63/19.46 ppm (^{1}H/^{13}C) assigned to methynic and methylenic groups of DACH, respectively.

The [^{1}H, ^{15}N] HSQC 2D spectrum of compound **3** shows only one cross-peak at 7.92/23.82 ppm (^{1}H/^{15}N). The ^{15}N chemical shift (23.82 ppm) is at higher field than in other Pt(IV) complexes with similar coordination environment ($PtN_2Cl_2O_2$) and having an aliphatic diamine as chelate ligand.[29,33] We think that the deshielding of the nitrogen atoms could be a consequence of the steric constraints imposed by the bulky *cis*-1,4-DACH ligand and of the electron withdrawing effect of the DCA ligands in the axial positions.

Similar chemical shifts were observed in the other Pt(IV) derivative with axial DCA ligands investigated in this work (*cis*,*trans*,*cis*-[Pt(OXA)(DCA)$_2$(*cis*-1,4-DACH)], **6**; Experimental Section and Supporting Information).

Solution behavior of *cis,trans,cis*-[$PtCl_2$(DCA)$_2$(*cis*-1,4-DACH)] (3).

It is generally assumed that Pt(IV) pro-drugs escape reaction with nucleophiles in the blood, so that they can reach the tumor unaltered and, once inside the cells, can be activated by reduction thereby releasing the cytotoxic Pt(II) species and the two axial ligands.[9,34,35] However, this is not always the case and Pt(IV) complexes with haloacetato ligands in the axial positions can undergo rather fast hydrolysis under biologically relevant conditions with a stepwise release of two molecules of haloacetate and final formation of a Pt(IV) dihydroxido species. In particular, HPLC analysis of water solutions (pH 7, 37 °C) of *cis*,*trans*,*cis*-[Pt(OXA)(TFA)$_2$(*1R*,*2R*-DACH)] (TFA = Trifluoroacetate), *cis*,*trans*,*cis*-[Pt(OXA)(DCA)$_2$(*1R*,*2R*-DACH)], and *cis*,*trans*,*cis*-[$PtCl_2(DCA)_2(NH_3)_2$] (mitaplatin) revealed that these compounds undergo hydrolysis with half lives of 6, 180, and 120 minutes, respectively.[32] Therefore, since *in vitro* cytotoxicity studies usually require 24-96 hours incubation times, it is very likely that these compounds with haloacetates undergo hydrolysis in the extracellular medium of the cancer cells. Nevertheless, mitaplatin,[19] *cis*,*trans*,*cis*-[Pt(OXA)(DCA)$_2$(*1R*,*2R*-DACH)],[36] and *cis*,*trans*,*cis*-[Pt(OXA)(TFA)$_2$(*1R*,*2R*-DACH)][37] proved to be very active in a variety of cancer cell lines.

Hence, the stability of complex **3** was investigated by ^{1}H-NMR in deuterated aqueous, phosphate buffered, saline solution (7.87 mM, pH 7.4 in DMSO-d_6/D_2O ratio of 10:90 (V/V)) at 37 °C. The spectrum acquired soon after dissolving the sample shows only the peak of coordinated DCA located at 6.25 ppm (marked with ✖ in Figure 4). After 30 minutes of incubation we observed the decay of the peak at 6.25 ppm and the concomitant increase of a peak resonating at 5.86 ppm (●, Figure 4) which was assigned to free DCA by comparison with a sample of pure DCA in the same experimental conditions ([^{1}H-^{13}C]-HSQC 2D NMR, not shown). The spectra recorded after 1 and 2 h showed the decrease of the signal of coordinated DCA to 45% and 24%, respectively, and its complete disappearance after 3 hours. The half-life of **3**, monitored by ^{1}H-NMR spectroscopy, was approximately 60 min, a value quite similar to that reported for mitaplatin (45 min) in D_2O at pH = 7, but lower than that found, in cell culture medium, for *cis*,*trans*,*cis*-[Pt(OXA)(DCA)$_2$(*1R*,*2R*-DACH)] (209 min) which, however, has an oxalate and a different isomer of DACH as ligands.[38]

In a recent paper,[36] it was suggested that even if Pt(IV) derivatives such as *cis*,*trans*,*cis*-[Pt(OXA)(DCA)$_2$(*1R*,*2R*-DACH)] tend to hydrolyze to a certain extent before entering the tumor cells, it is possible that also the hydrolysis products may accumulate readily in the cells.

Unlike other Pt(IV) derivatives of kiteplatin, which could undergo spontaneous reduction to Pt(II),[30] no spontaneous reduction was detected by ^{1}H-NMR in the present case.

Reduction of *cis*,*trans*,*cis*-[PtCl$_2$(DCA)$_2$(*cis*-1,4-DACH)] (3) by ascorbic acid/sodium ascorbate.

The ^{1}H-NMR spectra, recorded at different times, are reported in Figure 5. Soon after mixing of the reactants, a peak located at 6.36 ppm indicates coordinated DCA in the starting complex **3** (marked with ★ in Figure 5), while the additional signal appearing at 5.92 ppm indicates free DCA (marked with ● in Figure 5). In the following 20 minutes at 25 °C an increase of free DCA was noted. After additional 45 minutes at 37 °C only free DCA was present. Meanwhile, the singlet (with Pt satellites) of the methynic protons of coordinated *cis*-1,4-DACH, at 3.38 ppm in complex **3**, had shifted to 3.30 ppm and small changes had also affected the region of the methylenic protons of *cis*-1,4-DACH (2.00 - 1.60 ppm). The latter features are in accord with reduction of complex **3** to **1**.

Reduction of *cis*,*trans*,*cis*-[PtCl$_2$(OH)$_2$(*cis*-1,4-DACH)] (2) by ascorbic acid in phosphate buffer.

Since **3** can undergo hydrolysis affording **2**, we have investigated also the reduction of **2** by ascorbic acid in phosphate buffer (Figure S3 in Supporting Information). Starting from complex **2** (peaks marked with ▲ in Figure S3), after 50 minutes at 37 °C there was the formation of a yellow precipitate while the spectrum of the solution showed a decrease of the signals of **2** located at 6.37 and 1.84 ppm (NH_2 and CH_2, respectively) and a new signal at 1.72 ppm (marked with ♦ in Figure S3) assigned to the methylenic protons of coordinated DACH in a new species. In the following 3 h the signal located at 1.72 ppm increased in intensity while the signals at 6.37 and 1.84 ppm

disappeared completely (the methynic protons underwent only a small shift from 3.22 to 3.19 ppm). The solution was separated, taken to dryness under vacuum, then the solid residue was dissolved in DMSO-d_6 and analyzed by ^{1}H-NMR. Apart from the signals of ascorbic acid, the only other signals present were those typical of kiteplatin. Also the yellow precipitate was isolated, washed with water, and analyzed by ^{1}H-NMR in DMSO-d_6; it proved to be the Pt(II) species kiteplatin (data not shown).

Therefore, we conclude that also compound **2** can be easily reduced to kiteplatin by ascorbic acid.

Cytotoxicity.

The *in vitro* antitumor activity of **1**−**6** was evaluated and compared to that of the reference metallo-drugs cisplatin (CDDP) and oxaliplatin (OXP) as well as to that of DCA (compound **1** had already proved to be endowed with an excellent antineoplastic efficacy).[25] Cell lines representative of colon (HCT-15), lung (A549), breast (MCF-7), pancreatic (BxPC3) and cervical (A431) cancers, along with melanoma (A375), were used and the cytotoxicity was evaluated by means of the MTT test after 72 h of treatment. IC_{50} values, calculated from dose-survival curves, are reported in Table 1. Cytotoxic activity against BxPC3 cells was also assessed by means of SRB test (see Supporting Information Figure S4) and results were consistent with those collected by MTT test.

According to previous data, kiteplatin exhibited very similar antiproliferative activity for all tested cancer cells, with IC_{50} values comparable to those of OXP and about 3-fold smaller than those recorded for CDDP.[25] Compound **2** proved to be less effective with mean IC_{50} values exceeding 3 and 8 times those recorded for CDDP and OXP, respectively. These data are in accord with previous studies performed on L1210 murine leukemia and A2780 human ovarian cancer cells,[28] where the low cytotoxicity of **2** was correlated to its highly negative reduction potential.[39]

Compound **3**, with axial DCA ligands, elicited a cytotoxicity rather similar to those of OXP and kiteplatin (mean IC_{50} values of 3.1, 2.9, and 2.7 μM for **3**, kiteplatin, and oxaliplatin, respectively). Interestingly, compound **3** induced against the human pancreatic carcinoma cells BxPC3 an

antiproliferative effect that was 6 and 2.5 times greater than those of CDDP and OXP, respectively. A similar relationship was found among compounds **4**, **5**, and **6** which differ from **1**, **2**, and **3** by having an oxalate in place of two chlorido ligands in the equatorial plane. However, in general, the set of compounds **4**-**6** was less effective than compounds **1**-**3**. Thus, compound **4** has average IC_{50} value approximatively 4-fold higher than those of OXP and kiteplatin. Compound **5**, bearing two hydroxido ligands in the axial positions, was much less effective than the parental Pt(II) compound **4**. Finally, compound **6** had a cytotoxicity profile comparable to that of **4**.

The cell growth inhibition elicited by all derivatives was found to be strictly time-dependent (see Supporting Information Figure S5).

It is important to note that both Pt(IV)-DCA complexes (**3** and **6**) were significantly more effective than free DCA. The modest antiproliferative activity of DCA is explained taking into account that, being ionized in physiological solutions, it barely crosses the plasma membrane by passive diffusion, thus accumulating very scarcely inside the cell.[36,40]

Interestingly, by comparing the cytotoxicity data obtained with compounds **3** and **6** against A549 and MCF-7 cell lines with those previously reported by Lippard and coworkers for Mitaplatin,[19] it comes out that the DCA-kiteplatin derivatives are more effective than Mitaplatin. Actually, the IC_{50} values (μM) calculated on A549 cells for Mitaplatin and compounds **3** and **6** are 14, 3.2 and 11.3, respectively, whereas on MCF-7 human breast carcinoma cells are 18.0, 4.7, and 12.5 for Mitaplatin and compounds **3** and **6**, respectively.

In order to allow a more complete comparison between the *in vitro* antitumor potentials of **3** and Mitaplatin, we have tested the kiteplatin-DCA derivative **3** also against HeLa and U2-OS cells, which had been included in the cancer cell line panel used to test the activity of Mitaplatin.[19] As it is clearly evident from Table 2, complex **3** showed IC_{50} values about 3 and 1.5 times lower than those elicited by Mitaplatin against osteosarcoma U2-OS and cervical HeLa cancer cells, respectively.

Moreover, a comparison between the cytotoxicity of complex **6** and that of the analogous complex *cis*,*trans*,*cis*-[Pt(OXA)(DCA)$_2$(*1R*,*2R*-DACH)] is possible only against the MCF-7 tumor cell line where the IC_{50} values (μM) resulted to be, respectively, 12.6 and 1.6.[36]

The antiproliferative activity of Pt(II,IV) complexes was also investigated in two pairs of additional cell lines, including cisplatin-resistant human ovarian adenocarcinoma C13* cells and oxaliplatin-resistant human colon carcinoma LoVo-OXP cells. Multiple mechanisms are known to underlie the resistance to CDDP of C13* cells; these involve (i) reduced intracellular drug accumulation,[41] (ii) high cellular levels of glutathione and metallothioneins,[42] (iii) enhanced repair of platinum-DNA adducts,[43] and (iv) overexpression of the Trx system.[44] On the other hand, OXP resistant cells are mainly characterized by reduced drug accumulation and raised thiol levels whereas increased tolerance to DNA platination seems to be less evident.[45]

Cytotoxicity was assessed after 72 h of drug treatment by MTT test and the IC_{50} and RF values (RF = resistance factor, defined as the ratio between IC_{50} of resistant cells over IC_{50} of sensitive ones) are reported in Table 3. In line with previous results,[25] all new compounds exhibited similar cytotoxic potency both on cisplatin-sensitive and on cisplatin-resistant cells. Moreover, with the only exception of compound **4**, Pt(II,IV) derivatives proved to be capable of overcoming also the OXP resistance. These results strongly confirm the effectiveness of the Pt(1,4-DACH) scaffold to circumvent oxaliplatin resistance in LoVo colon cancer cells. The partial cross-resistance of compound **4** could be attributed to the presence of the oxalato ligand, which could function as MRP substrate and accentuate the drug efflux from cells.[46]

The cytotoxicity of Pt(IV)-DCA derivatives **3** and **6** was also evaluated against non-tumor cells, namely human lung fibroblasts MRC-5 cells and human embryonic kidney HEK293 cells (Table 4). Compound **6** elicited a cytotoxic activity similar to or lower than that exerted by CDDP, whereas compound **3** was significantly more cytotoxic than cisplatin in HEK293. However, in all cases the selectivity index (SI = ratio between average IC_{50} of non-tumor cells and IC_{50} of malignant cells) calculated for complexes **3** and **6** was higher than that calculated for cisplatin (SI of 3.5, 3.1, and 2.1

for **3**, **6**, and CDDP, respectively), attesting the preferential cytotoxicity of both Pt(IV)-DCA complexes towards neoplastic cells.

Cellular uptake and DNA binding

The antiproliferative activity of platinum-based anticancer agents deeply relies on cellular uptake as well as DNA binding and transcription inhibition.[47] Therefore we investigated the cellular uptake and DNA binding of all tested compounds in human BxPC3 pancreatic cancer cells. Cells were treated for 24 h with the tested compounds (concentration 5 μM) and the total cellular and the DNA-bound platinum contents were quantified by GF-AAS analysis. The results, expressed as pg metal/10^6 cells, are summarized in Figure 6. Both Pt(IV) derivatives bearing hydroxido ligands in the axial positions (**2** and **5**) were the worst in crossing the cell plasmalemma. Interestingly, the cellular internalization of **3** was significantly higher than that of the parental Pt(II) complex **1** whereas it was similar for compounds **4** and **6**.

Concerning the DNA-platination levels, the least effective complexes were the Pt(IV) derivatives with hydroxido ligands, the same for which the cellular accumulation was the lowest. Compound **1** (kiteplatin) gave the highest degree of DNA platination whereas for compound **3**, in spite of its greater cellular accumulation, the amount of platinum bound to DNA was low. An opposite trend was observed in the pair of compounds **4** and **6** where the Pt(IV) species with DCA ligands gave higher degree of DNA platination than the Pt(II) counterpart. Taken together, these data indicate that while for Pt(II) derivatives the cytotoxicity data well correlate with both cellular uptake and DNA platination (Figure 6), this is not the case for Pt(IV)-DCA complexes. For instance, in the case of **3**, a major cellular uptake with respect to the parental Pt(II) complex, did not correspond to enhanced DNA platination levels, however, the Pt(IV) derivative retained a cytotoxicity profile resembling that of the parental Pt(II) complex. These data strongly support the hypothesis that different targets could account for the antiproliferative effects of Pt(IV)-DCA compounds.

Effect on mitochondria.

Based on the above finding of high cytotoxicity of Pt(IV)-DCA compounds and taking into consideration that DCA can affect PDK, we investigated the effects of Pt(IV)-DCA derivatives **3** and **6** on mitochondria. In particular, we investigated the ROS production, the alteration of the mitochondrial membrane potential, and the functioning of the respiratory chain.

Treatment of BxPC3 cells with derivatives **3** and **6** determined a substantial increase in cellular ROS production, both in a dose- and time-dependent manner (Figure 7, panel A). Remarkably, after 2 h treatment with compound **3**, the hydrogen peroxide content was up to 3.5 times greater than that obtained with antimycin, a classical inhibitor of the mitochondrial respiratory chain at the level of complex III. Reduction of Pt(IV) complexes is *per se* responsible of ROS formation, however, the conspicuous increase of cellular basal ROS production could be also induced by inhibition of the peroxidase systems as well as by a direct effect on oxidative phosphorylation (OXPHOS). Indeed, derivatives **3** and **6** showed to be capable of hampering OXPHOS (Figure 7, panel B), thus determining a reduction of O_2 consumption. OXPHOS blockage and consequent increase of ROS production led to hypopolarization of the mitochondrial membrane and swelling. Consistently, a significant time and dose-dependent increase of cells with depolarized mitochondria was observed after treatment with **3** and **6** (Figure 7, panel C).

Morphological analyses by TEM of BxPC3 cells treated with both Pt(IV)-DCA derivatives showed disrupted cristae and significant increase in volume (swelling) with respect to control cells, confirming that **3** and **6** elicit an "antimitochondrial" effect (Figure 8).

Monitoring of cellular thiols and glutathione status.

Cells are equipped with various enzymatic and nonenzymatic antioxidant systems to contrast ROS/RNS and maintain redox homeostasis.[48] Nonenzymatic antioxidants, executing thiol–disulfide exchange reactions, play a major role in maintaining cellular redox balance and, among them, GSH is the most abundant. In many cases, oxidant-induced GSH/GSSG and SH/SS imbalance has been

found to precede loss of the mitochondrial integrity, caspase-3 activation, and apoptotic bodies formation.[49] Therefore, in order to highlight the nature of the cellular stress determined by Pt(IV) complexes, cellular thiols and glutathione status were monitored.

Pt(IV)-DCA complexes were not found to alter the thiol and GSH redox homeostasis of BxPC3 cells after 12 or 24 h treatment (data not shown). However, after 48 h incubation with 12.5 μM concentration of Pt(IV)-DCA derivatives, an increase of oxidized glutathione (GSSG) was detected (Figure 9, panel B, insert b) without substantial change of total sulfhydryl content (Figure 9, panel A) and total GSH level (Figure 9, panel B). In contrast, both compounds caused a substantial activation of caspase-3/7 (Figure 10, panel A). Already after 24 h of incubation with IC_{50} of **3**, caspase-3/7 cleavage was similar to that induced by staurosporin, a well-known caspase-dependent apoptosis inducer. Furthermore, treatment with zVAD, a cell-permeable pan-caspase inhibitor, strongly decreased the caspase-3/7 activation, thus confirming the role played by these proteases in cancer cell death induced by Pt(IV)-DCA derivatives. Hoechst staining of BxPC3 cells after 48 h incubation with Pt(IV)-DCA derivatives clearly indicated the occurrence of nuclear condensation (pyknosis) and blebbing (Figure 10, panel B).

***In vivo* studies.**

Compound **3** was evaluated for its *in vivo* activity in the murine LLC solid tumor. The tumor growth inhibition induced by complex **3** was compared to that promoted by CDDP. Seven days after tumor inoculation, tumor-bearing mice were randomized into vehicle control and treatment groups (5 mice per group). Control mice received the vehicle (0.5 % DMSO (v/v) and 99.5% of a saline solution (v/v)), whereas treated groups received daily doses of **3** (1.5 $mg \cdot kg^{-1}$ in a vehicle solution composed of 0.5 % DMSO (v/v) and 99.5% of saline solution (v/v)) or cisplatin (1.5 $mg \cdot kg^{-1}$ in saline solution). Tumor growth was estimated at day 15, and the results are reported in Table 5. As an indication of the adverse side effects, changes in the body weights of tumor-bearing mice were monitored every two days (Figure 11). Noteworthy, administration of **3** induced a 81%

reduction of the tumor mass compared to that of the control group. A similar effect was exerted by CDDP (80% reduction), however, the time course of body weight changes indicates that CDDP induces elevated anorexia, while treatment with **3** results in a body weight loss <10% (Figure 11).

Conclusions

The aim of this work was to develop multitarget therapeutic agents for the treatment of multifactorial diseases. Thus, new platinum(IV) derivatives of kiteplatin having two dichloroacetate (an inhibitor of the pyruvate dehydrogenase kinase) in axial positions were synthesized, characterized, and tested *in vitro* against a series of tumor cell lines and *in vivo*.

Among the Pt(IV) derivatives investigated, the most active (**3**) was found to undergo quite rapid transformation in solution (pH = 7.4) with hydrolysis of the axial DCA ligands. The reduction of compound **3** and of the corresponding solvated species (**2**) by ascorbic acid to the Pt(II) counterpart (kiteplatin) was fast for both complexes (half times of minutes). Notwithstanding the rather fast hydrolysis in PBS, the Pt(IV) kiteplatin derivatives investigated in this study displayed potent pharmacological benefits, the results paralleling previously published data on mitaplatin.

The possible role of DCA released by the Pt(IV) compounds in eliciting the antiproliferative activity was investigated. Compounds **3** and **6** led to a substantial increase of ROS production, blockage of oxidative phosphorylation, hypopolarization of the mitochondrial membrane, and caspase-3/7-mediated apoptotic cell death. In summary, the fast hydrolysis of **3** (and formation of the hydroxido species) is not such to decrease the cellular uptake of this compound which, instead, is about 30% greater than that of the Pt(II) counterpart (**1**) and much greater (nearly 8 times) than that of the di-hydroxido species (**2**). However, the greater cellular accumulation of **3** does not result in greater DNA-platination, which remains much lower than that of **1** (about 4 times) and only slightly higher than that of **2** (roughly 1.6 times). This supports the notion that the antitumor activity of **3** (comparable to that of **1** and greater than that of **2**) probably involves, in addition to the DNA damage, also a protein dependent pathway as shown by substantial increase of ROS production,

blockage of oxidative phosphorylation, hypopolarization of the mitochondrial membrane, and caspase-3/7-mediated apoptotic cell death. The red-ox activity of Pt(IV) species and the dichloroacetate-dependent inhibition of the pyruvate dehydrogenase kinase could also contribute to this DNA damage-independent pathway.

Compound **3** was particularly active against human pancreatic carcinoma cells and both compounds **3** and **6** showed a preferential cytotoxicity versus neoplastic cells rather than non-tumor cells. In general, the use of oxalate as leaving ligand seems to reduce the cytotoxicity of kiteplatin derivatives.

Both Pt(II) and Pt(IV) derivatives of kiteplatin (with the only exception of **4**) proved to overcome oxaliplatin-resistance; this result is particularly important in view of the fact that the metastatic colorectal cancer is the third most common cancer in males and the second in females,[50] and inevitably resistance to oxaliplatin is developed. Therefore, there is a compelling need to develop new platinum-based drugs capable to overcome oxaliplatin resistance or intolerance.

Finally, *in vivo* results obtained on LLC showed that **3** exerts a reduction of tumor mass similar to that of cisplatin but it is less toxic.

The overall results presented in this work indicate that compound **3** could be an ideal candidate for clinical trials in particular for the treatment of pancreatic tumor or oxaliplatin-resistant colorectal cancer. Moreover, since *cis*-1,4-DACH increases water-solubility of the Pt(IV) compounds with respect to 1,2-DACH, the Pt(IV) derivatives of *cis*-1,4-DACH could be better suited for oral administration, this will be performed in a future investigation.

Experimental

Materials and methods

Commercial reagent grade chemicals and solvents were used as received without further purification. ^{1}H-NMR and [^{1}H-^{195}Pt] HSQC spectra were recorded on a Bruker Avance DPX 300

MHz instrument. [^{1}H-^{13}C]-HSQC and [^{1}H, ^{15}N]-HSQC (natural abundance ^{15}N) 2D NMR spectra were recorded on a Bruker Avance III 700 MHz instrument. ^{1}H and ^{13}C chemical shifts were referenced using the internal residual peak of the solvent (DMSO-d_6: 2.50 ppm for ^{1}H and 39.51 ppm for ^{13}C). ^{15}N chemical shifts were referenced to external $^{15}NH_4Cl$ (1M in HCl 1M) placed at 24 ppm with respect to liquid NH_3.[51] ^{195}Pt NMR spectra were referenced to K_2PtCl_4 (external standard placed at −1620 ppm with respect to $Na_2[PtCl_6]$).[52]

Electrospray ionisation mass spectrometry (ESI-MS) was performed with an electrospray interface and an ion trap mass spectrometer (1100 Series LC/MSD Trap system Agilent, Palo Alto, CA).

Elemental analyses were carried out with an Eurovector EA 3000 CHN instrument.

Kiteplatin (**1**),[53] *cis,trans,cis*-[$PtCl_2(OH)_2$(*cis*-1,4-DACH)] (**2**),[30] and [Pt(OXA)(*cis*-1,4-DACH)] (**4**; OXA = oxalate)[28] were prepared according to already reported procedures.

Synthesis of *cis,trans,cis*-[$PtCl_2(DCA)_2$(*cis*-1,4-DACH)] (3; DCA = HCl_2CCOO^-). To a suspension of **2** (43 mg, 0.104 mmol) in 2 mL of tetrahydrofuran (THF) was added dichloroacetic anhydride (125 μL, 196.7 mg, 0.82 mmol) and the reaction mixture was stirred in the dark at room temperature for 17 h. *n*-Pentane was added to the yellow solution to precipitate a light yellow solid that was isolated by filtration of the mother liquor, washed with n-pentane and a small amount of ice cold water (200 μL) and dried under vacuum. Yield 62% (41 mg, 0.064 mmol). *Anal.: calculated for* $C_{10}H_{16}Cl_6N_2O_4Pt$ (**3**): C, 18.88; H, 2.54; N, 4.40%. *Found:* C, 18.76; H, 2.58; N, 4.35%. ESI-MS: *calculated for* $C_{10}H_{16}Cl_6N_2O_4PtNa$ [**3**+Na]$^+$: 658.9. *Found: m/z* 658.7. ^{1}H NMR (DMSO-d_6): 7.92 (4H, NH_2), 6.58 (2H, CH_d; see Scheme 1 for numbering of protons), 3.03 (2H, CH_a), 1.63 (8H, $CH_{b/c}$) ppm. ^{195}Pt NMR (DMSO-d_6): 1196.30 ppm. ^{13}C NMR (DMSO-d_6): 65.40, 50.10, 19.46 ppm. ^{15}N NMR (DMSO-d_6): 23.82 ppm.

Synthesis of *cis*,*trans*,*cis*-[Pt(OXA)(OH)$_2$(*cis*-1,4-DACH)] (5; OXA = oxalate). Briefly, a solution of [Pt(OXA)(*cis*-1,4-DACH)] (**4**) (170 mg, 0.428 mmol) in 17 mL of H_2O was treated with a solution of H_2O_2 in H_2O (30% w/w, 855 μL). The mixture was stirred at room temperature for 24 h in the dark. The resulting suspension was concentrated under reduced pressure to a minimum volume. Addition of acetone induced the formation of a white precipitate that was isolated by filtration of the mother liquor, washed with acetone, and dried under vacuum. Yield 83% (151 mg, 0.35 mmol). *Anal.: calculated for* $C_8H_{16}N_2O_6Pt \cdot 0.5H_2O$ (**5**$\cdot 0.5H_2O$) C, 21.82; H, 3.89; N, 6.36 %. *Found*: C, 21.83; H, 3.94; N, 6.13 %. ESI-MS: *calculated for* $C_8H_{16}N_2O_6PtK$ [**5**+K]$^+$ 470.39. *Found :* $^m/_z$ 470.03. ^{1}H-NMR (DMSO-d_6): 6.71 (4H, NH_2), 2.91 (2H, CH_a), 1.97 (4H, CH_b), 1.50 (4H, CH_c), 0.77 (2H, OH) ppm (see Scheme 1 for numbering of protons).

Synthesis of *cis*,*trans*,*cis*-[Pt(OXA)(DCA)$_2$(*cis*-1,4-DACH)] (6). To a suspension of *cis*,*trans*,*cis*-[Pt(OXA)(OH)$_2$(*cis*-1,4-DACH)] (**5**) (100 mg, 0.23 mmol) in 7 mL of THF was added dichloroacetic anhydride (283 μL, 1.85 mmol) and the reaction mixture was stirred in the dark at room temperature for 17 h. The resulting white precipitate was isolated by filtration, washed with *n*-pentane and dried under vacuum. Yield 75.6% (117.3 mg, 0.18 mmol). *Anal.: calculated for* $C_{12}H_{16}Cl_4N_2O_8Pt$ (**6**) C, 22.07; H, 2.47; N, 4.29 %. *Found*: C, 22.46; H, 2.73; N, 4.44 %. ESI-MS: *calculated for* $C_{12}H_{15}Cl_4N_2O_8Pt$ [**6**-H]$^-$ 650.92 *Found:* $^m/_z$ 650.93.

^{1}H-NMR (DMSO-d_6): 7.69 (4H, NH_2), 6.53 (2H, CH_d), 2.98 (2H, CH_a), 1.72 (8H, $CH_{b/c}$) ppm (see Scheme 1 for numbering of protons).

Stability of *cis*,*trans*,*cis*-[PtCl$_2$(DCA)$_2$(*cis*-1,4-DACH)] (3) in PBS.

The solution behavior of **3** was investigated by ^{1}H-NMR spectroscopy. Complex **3** (0.5 mg, 0.786 μmol) was dissolved in DMSO-d_6 (0.5 mL). 100 μL of the previous solution were diluted with 900 μL of a deuterated aqueous phosphate buffered saline solution (7.87 mM, pH 7.4) obtaining a final

concentration of 157 μM (DMSO-d_6/D_2O, 10:90 (V/V)). The sample was incubated at 37 °C in the dark and ^{1}H-NMR spectra recorded at different time intervals.

Reduction of *cis,trans,cis*-[$PtCl_2(OH)_2$(*cis*-1,4-DACH)] (2) by ascorbic acid.

Cis,trans,cis-[$PtCl_2(OH)_2$(*cis*-1,4-DACH)] (**2**) (4.97 mg, 12 μmol) was dissolved in deuterated phosphate buffer (H_2O/D_2O, 90:10 v/v, 500 μL; 100 mM NaCl; 200 mM Na_2HPO_4/NaH_2PO_4, pH 7.0) and placed into a NMR tube. A threefold excess of ascorbic acid (6.34 mg, 36 μmol) dissolved in the same buffer (100 μl), was added into the NMR tube and the resulting solution, kept at 37 °C, was monitored by recording ^{1}H-NMR spectra at different time intervals.

Reduction of *cis,trans,cis*-[$PtCl_2(DCA)_2$(*cis*-1,4-DACH)] (3) by ascorbic acid/sodium ascorbate.

Cis,trans,cis-[$PtCl_2(DCA)_2$(*cis*-1,4-DACH)] (**3**) (3.1 mg, 4.87 μmol) was dissolved in Acetone-d_6 (550 μl), and placed into a NMR tube to acquire ^{1}H NMR. A fivefold excess of ascorbic acid (4.3 mg, 24.3 μmol) and fivefold excess of sodium ascorbate (4.81 mg, 24.3 μmol) dissolved in D_2O (100 μl) were added into the NMR tube and the resulting solution was monitored by recording ^{1}H-NMR spectra at different time intervals while the sample was kept at 25 °C for the first 20 minutes and then at 37 °C for 45 minutes.

Experiments with cultured human cells.

Pt(IV) compounds **2**, **3**, **5**, and **6** were dissolved in DMSO just before running the experiment and a calculated amount of drug solution was added to the cell growth medium to a final DMSO concentration of 0.5%, which had no detectable effect on cell viability. Cisplatin and Pt(II) compounds **1** and **4** were dissolved in 0.9% NaCl solution.

Cell cultures.

Human breast (MCF-7), colon (LoVo and HCT-15), lung (A549), cervical (HeLa) and pancreatic (BxPC3) carcinoma cell lines together with melanoma (A375) cells, non-transformed embryonic kidney cells (HEK293), and lung fibroblasts (MRC-5) were obtained from American Type Culture Collection (ATCC, Rockville, MD). The human ovarian cancer cell line 2008 and its cisplatin resistant variant, C13*, were kindly provided by Prof. G. Marverti (Dept. of Biomedical Science of Modena University, Italy). Human cervical carcinoma (A431) cells and the human osteosarcoma cell line (U-2 OS), were kindly provided by Prof. F. Zunino (Division of Experimental Oncology B, Istituto Nazionale dei Tumori, Milan, Italy). The LoVo-OXP cells were derived, using a standard protocol, by growing LoVo cells in increasing concentrations of oxaliplatin and following nine months of selection of resistant clones, as previously described.[54] Cell lines were maintained in the logarithmic phase at 37 °C in a 5% carbon dioxide atmosphere using the following culture media containing 10% fetal calf serum (Euroclone, Milan, Italy), antibiotics (50 units/mL penicillin and 50 μg/mL streptomycin) and 2 mM L-glutamine: (i) RPMI-1640 medium (Euroclone) for 2008, C13*, MCF-7, HCT-15, A431 and BxPC3 cells; (ii) F-12 HAM'S (Sigma Chemical Co.) for A549, HeLa, LoVo, and LoVo-OXP cells; iii) DMEM (Sigma Chemical Co.) for A375 and HEK293 cells; iv) MEM for MRC-5 cells; v) McCoy's (Euroclone, Milan, Italy) medium, supplemented with 0.1% gentamicin for U-2 OS cells.

Cytotoxicity assays.

The growth inhibitory effect toward tumor cells was evaluated by means of the MTT assay. Briefly, (3 - 8) x 10^3 cells/well, dependent upon the growth characteristics of the cell line, were seeded in 96-well microplates in growth medium (100 μL). After 24 h, the medium was removed and replaced with fresh media containing the compound to be studied at the appropriate concentration. Triplicate cultures were established for each treatment. After 24, 48, or 72 h, each well was treated with 10 μL of a 5 mg/mL MTT saline solution and, after 5 h of incubation, 100 μL of a sodium dodecylsulfate (SDS) solution in 0.01 M HCl were added. After an overnight incubation, cell

growth inhibition was detected by measuring the absorbance of each well at 570 nm using a Bio-Rad 680 microplate reader. The mean absorbance for each drug dose was expressed as a percentage of the control, untreated, well absorbance and plotted vs drug concentration. The IC_{50} values, the drug concentrations that decrease the mean absorbance at 570 nm to 50% of that of untreated control wells, were calculated from the dose–response curves with the four-parameter logistic model (4PL). The final value is the mean ± S.D. of at least three independent experiments performed in triplicate.

Cellular accumulation of Pt.

BxPC3 cells ($2 \cdot 10^6$) were seeded in 75 cm^2 flasks in growth medium (20 mL). After 24 h, the medium was replaced and the cells incubated for 24 h in the presence of the tested complexes. Cells monolayers were washed twice with cold phosphate-buffered saline (PBS), harvested and counted. Samples were subjected to three freeze-thaw cycles at −80 °C, and then vigorously vortexed. The samples were treated with highly pure nitric acid (1 mL; Pt≤0.01 $mg \cdot kg^{-1}$, Trace-SELECT Ultra, Sigma Chemical Co.) and transferred into a microwave teflon vessel. Subsequently, samples were submitted to standard mineralization procedures. Samples were analyzed for platinum by using a Varian AA Duo graphite furnace atomic absorption spectrometer (Varian, Palo Alto, CA; USA) at the wavelength of 324.7 nm. The calibration curve was obtained using known concentrations of standard solutions purchased from Sigma Chemical Co.

Cellular thiols.

BxPC3 cells ($5 \cdot 10^5$) were seeded in 6-well plates in growth medium (4 mL). After 24 h, cells were incubated for 24 and 48 h with increasing concentrations of tested complexes. Subsequently, the thiol content was measured as previously described.[55]

Total and oxidized intracellular glutathione.

BxPC3 cells ($3.5 \cdot 10^5$) were seeded in 6-well microplates in growth medium (4 mL). Following 24 and 48 h exposure with tested complexes at increasing concentrations, cells were washed twice with PBS, treated with 6% metaphosphoric acid and scraped. Samples were centrifuged and the supernatants were neutralized with Na_3PO_4 and assayed for total and oxidized glutathione following the procedure reported by Bindoli *et al*.[56] Aliquots of pellets were dissolved in RIPA buffer and the protein content was determined.

ROS production.

The production of ROS was measured in BxPC3 cells (10^4 per well) grown for 24 h in 96-well plates in RPMI medium without phenol red (Sigma Chemical Co.). Cells were then washed with PBS and loaded with 10 μM 5-(and-6)-chloromethyl-2′,7′-dichlorodihydrofluorescein diacetate, acetyl ester (CM–H_2DCFDA; Molecular Probes-Invitrogen) for 25 min, in the dark. Afterwards, cells were washed with PBS and incubated with increasing concentrations of tested complexes. Fluorescence increase was estimated with a plate reader (Fluoroskan Ascent FL, Labsystem, Finland) at 485 (excitation) and 527 nm (emission). Antimycin (3 μM, Sigma Chemical Co.), a potent inhibitor of Complex III in the electron transport chain, was used as positive control.

Mitochondrial membrane potential (ΔΨ).

The ΔΨ was assayed using the Mito-ID® Membrane Potential Kit according to the manufacturer's instructions (Enzo Life Sciences, Farmingdale, NY). Briefly, BxPC3 cells ($8 \cdot 10^3$ per well) were seeded in 96-well plates; after 24 h, cells were washed with PBS and loaded with Mito-ID Detection Reagent for 30 min at 37 °C in the dark. Afterwards, cells were washed with PBS and incubated with increasing concentrations of tested complexes. Fluorescence was estimated using a plate reader

(Fluoroskan Ascent FL, Labsystem, Finland) at 490 (excitation) and 590 nm (emission). Carbonylcyanide *m*-chlorophenyl hydrazone (CCCP, 4 μM), a chemical inhibitor of the oxidative phosphorylation, was used as positive control.

O_2 consumption.

The O_2 consumption was assessed using the Mito-ID® O_2 Extracellular Sensor Kit according to the manufacturer's instructions (Enzo Life Sciences, Farmingdale, NY). Briefly, BxPC3 cells ($15 \cdot 10^3$ per well) were seeded in 96-well plates. After 24 h, cells were treated with Mito-ID® O_2 Sensor Probe Solution containing the tested compounds at the appropriate concentration. Fluorescence was estimated using a plate reader (Fluoroskan Ascent FL, Labsystem, Finland) at 350 nm (excitation) and 610 nm (emission).

Transmission electron microscopy analyses.

About 10^6 BxPC3 cells were seeded in 24-well plates and, after 24 h incubation, were treated with the tested compounds and incubated for additional 24 h. Cells were then washed with cold PBS, harvested and directly fixed with 1.5% glutaraldehyde buffer with 0.2 M sodium cacodylate, pH 7.4. After washing with buffer and postfixation with 1% OsO_4 in 0.2 M cacodylate buffer, specimens were dehydrated and embedded in epoxy resin (Epon Araldite). Sagittal serial sections (1 μm) were counterstained with toluidine blue; thin sections (90 nm) were given contrast by staining with uranyl acetate and lead citrate. Micrographs were taken with a Hitachi H-600 electron microscope (Hitachi, Tokyo, Japan) operating at 75 kV. All photos were typeset in Corel Draw 11.

Hoechst 33258 staining.

BxPC3 cells were seeded into 8-well tissue-culture slides (BD Falcon, Bedford, MA, USA) at $5 \cdot 10^4$ cells/well (0.8 cm^2). After 24 h, cells were washed twice with PBS and following 48 and 72 h of treatment with IC_{50} doses of the tested compound, cells were stained for 5 min with 10 μg/mL of Hoechst 33258 (2'-(4-hydroxyphenyl)-5-(4-methyl-1-piperazinyl)-2,5'-bi-1H-benzimidazole trihydrochloride hydrate, Sigma–Aldrich) in PBS before being examined by fluorescence microscopy (Olympus).

Caspase-3 activation.

BxPC3 cells ($1 \cdot 10^6$) were treated for 24 h with the IC_{50} doses of tested compounds, harvested and homogenized in a lysis buffer [1% Triton X-100, 320 nM sucrose, 5 mM EDTA, 10 mM Tris–HCl and 2 mM DTT (1,4-dithio-DL-threitol) buffer (pH 7.6)]. Protein aliquots (100 μg) were stained at 37 °C for 60 min with fluorescent caspase-3 substrate *N*-Acetyl-Asp-Glu-Val-Asp-AMC (AMC = 7-amino-4-methylcoumarin) (Sigma Co.). Substrate hydrolysis was measured after 60 min by monitoring the release of AMC using a spectrofluorimeter (excitation at 370 nm, emission at 460 nm).

***In vivo* anticancer activity toward Lewis Lung Carcinoma (LLC).**

All studies involving animal testing were carried out in accordance with the ethical guidelines for animal research adopted by the University of Padua, acknowledging the Italian regulation and European Directive 2010/63/UE as to the animal welfare and protection and the related codes of practice. The mice were purchased from Charles River, Italy, housed in steel cages under controlled environmental conditions (constant temperature, humidity, and 12 h dark/light cycle), and alimented with commercial standard feed and tap water ad libitum. The LLC cell line was purchased from ECACC, United Kingdom. The LLC cell line was maintained in DMEM (Euroclone) supplemented

with 10% heat inactivated fetal bovine serum (Euroclone), 10 mM L-glutamine, 100 U mL^{-1} penicillin, and 100 $\mu g \cdot mL^{-1}$ streptomycin in a 5% CO_2 air incubator at 37 °C. The LLC was implanted intramuscularly (*i.m.*) as a 2×10^6 cell inoculum into the right hind leg of 8 week old male and female C57BL mice (24 ± 3 g body weight). After 7 days from tumor implantation (visible tumor), mice were randomly divided into 4 groups (5 animals per group) and subjected to daily *i.p.* administration of complex **3** (1.5 mg kg^{-1} dissolved in a vehicle solution composed of 0.5 % DMSO (v/v) and 99.5% of saline solution (v/v)), cisplatin (1.5 mg kg^{-1} in saline solution), or the vehicle solution (0.5 % DMSO (v/v) and 99.5% of saline solution (v/v)). At day 15, animals were sacrificed, the legs were amputated at the proximal end of the femur, and the inhibition of tumor growth was determined according to the difference in weight of the tumor-bearing leg and the healthy leg of the animals expressed as a percentage referring to the control animals. Body weight was measured every 2 days and was taken as a parameter for systemic toxicity. All reported values are the means ± SD of no less than three measurements. Multiple comparisons were made by the Tukey−Kramer test (**, $p < 0.01$; * or °, $p < 0.05$).

Statistical analysis.

All values are the means ± SD of no less than three measurements starting from three different cell cultures. Multiple comparisons were made by ANOVA followed by the Tukey−Kramer multiple comparison test (**$P < 0.01$; *$P < 0.05$), using GraphPad Software.

Acknowledgments

The Universities of Bari and Padova (Progetto di Ateneo CPDA121973/12; Italy), the Italian Ministero dell'Università e della Ricerca (MIUR), the European Union (COST CM1105 "Functional metal complexes that bind to biomolecules"), and the Inter-University Consortium for Research on the Chemistry of Metal Ions in Biological Systems (C.I.R.C.M.S.B.) are gratefully acknowledged.

Supporting Information available: NMR characterization of *cis,trans,cis*-[Pt(OXA)$(OH)_2$(*cis*-1,4-DACH)] (**5**) and *cis,trans,cis*-[Pt(OXA)$(DCA)_2$(*cis*-1,4-DACH)] (**6**) and reduction of *cis,trans,cis*-[$PtCl_2(OH)_2$(*cis*-1,4-DACH)] (**2**) with ascorbic acid. Sulforhodamine B assay and time-course cytotoxicity assay.

Table 1. ***In vitro*** **antitumor activity**

	IC_{50}(μM)±S.D.					
Compound	**HCT-15**	**A549**	**MCF-7**	**A375**	**A431**	**BxPC3**
kiteplatin, 1	2.7±0.9	5.5±0.4	3.0±1.1	1.9±0.8	1.5±0.9	3.9±0.8
2	10.3±1.4	39.8±0.8	13.6±6.4	6.2±2	6.3±2	38.9±5.5
3	3.2±1.1	3.2±1.8	4.7±1.2	3.0±1.3	3.0±1.0	1.7±0.9
4	12.2±1.8	6.4±1.6	10.3±2.4	12.1±1.6	7.1±3.2	5.5±2.2
5	>50	>50	>50	>50	>50	>50
6	13.7±3.8	11.0±1.4	12.6±1.3	4.99±1.15	7.41±2.11	17.75±4.65
CDDP	15.5±2.5	12.6±0.8	7.6±1.2	2.1±1.0	2.0±0.8	10.2±1.7
OXP	1.3±1.0	1.5±0.5	3.4±1.2	2.4±1.1	3.7±1.0	4.2±1.1
DCA	>50	>50	>50	>50	32.3±3.3	31.1±3.0

Cells ($3–8\times10^3$ mL^{-1}) were treated for 72 h with increasing concentrations of tested compounds. Cytotoxicity was assessed by MTT test. IC_{50} values were calculated by four parameter logistic model ($p < 0.05$). S.D. = standard deviation. CDDP = cisplatin; OXP = oxaliplatin; DCA = dichloroacetate.

Table 2. *In vitro* antitumor activity of Pt(IV) kiteplatin-DCA derivatives in comparison with Mitaplatin

	IC_{50}(μM)±S.D.			
Compound	**HeLa**	**U-2 OS**	**MCF-7**	**A549**
3	1.3±0.4	2.3±3.2	4.7±1.2	3.2±0.4
6	-	-	12.6±1.3	11.0±1.4
CDDP	1.1±0.1	5.1±1.1	7.6±1.2	12.6±0.8
Mitaplatin[a]	2.0	6.4	18	14

Cells ($3–8\times10^3$ mL^{-1}) were treated for 72 h with increasing concentrations of tested compounds. Cytotoxicity was assessed by MTT test. IC_{50} values were calculated by four parameter logistic model ($p < 0.05$). S.D. = standard deviation. CDDP = cisplatin. [a]Data from reference 19**.**

Table 3. Cross-resistance profiles

	IC_{50}(μM)±S.D.					
Compound	**2008**	**C13***	**R.F.**	**LoVo**	**LoVo-OXP**	**R.F.**
kiteplatin, 1	1.89±1.04	1.77±0.92	0.9	1.11±0.45	1.29±0.91	1.2
2	9.42±1.16	13.85±3.53	1.5	6.64±2.70	9.46±2.15	1.6
3	2.15±0.95	3.35±0.85	1.6	2.27±1.31	3.23±1.08	1.4
4	11.13±2.98	15.63±3.06	1.4	7.02±0.56	12.53±1.92	1.8
5	59.53±3.64	78.72±4.60	1.3	61.25±5.51	66.88±5.12	1.1
6	11.12±3.28	9.12±2.79	0.8	9.08±2.16	11.14±3.05	1.2
CDDP	2.26±1.06	23.73±2.42	10.5	7.63±1.53	13.13±2.47	1.7
OXP	1.65±1.01	3.33±1.84	2.0	1.45±1.91	23.49±2.63	16.2
DCA	>50	>50	-	>50	>50	-

Cells ($3–8\times10^4$ mL^{-1}) were treated for 72 h with increasing concentrations of tested compounds. Cytotoxicity was assessed by MTT test. IC_{50} values were calculated by four parameter logistic model ($p < 0.05$). S.D. = standard deviation. Resistant Factor (R.F.) is defined as IC_{50} resistant/parent line. CDDP = cisplatin; OXP = oxaliplatin; DCA = dichloroacetate.

Table 4. Cytotoxicity towards non-tumor cells.

Compound	IC_{50} [μM] ± S.D.	
	MRC-5	HEK293
3	17.23±1.98	4.45±1.98
6	46.73±3.84	23.75±3.15
CDDP	21.45±1.66	19.56±2.95

Cells ($5–8\times10^4$ mL^{-1}) were treated for 72 h with increasing concentrations of tested compounds. Cytotoxicity was assessed by MTT test. IC_{50} values were calculated by four parameter logistic model ($p < 0.05$). S.D. = standard deviation. CDDP = cisplatin.

Table 5. ***In vivo*** **antitumor activity**

Compound	Daily dose ($mg \cdot kg^{-1}$)	Average tumor weight (mean±S.D., g)	Inhibition of tumor growth (%)
control[a]	-	0.397±0.07	-
3	1.5	0.073±0.04	81.61
CDDP	1.5	0.076±0.02	80.86

[a]Vehicle: DMSO (0.5%, v/v) and 0.9% NaCl water solution (99.5%, v/v). Lewis lung carcinoma (LLC) was implanted i.m. ($2 \cdot 10^6$ cells inoculum) into the right hind leg of 8-week old male and female C57BL mice (24 ± 3 g body weight). Chemotherapy was delayed until the tumor became visible (day 7). Day 7-14: animal received 1.5 mg/kg of **3** or cisplatin daily i.p.. At day 15 animals were sacrificed, legs amputated at the proximal end of the femur, and the inhibition of tumor growth was determined as the difference in weight of the tumor-bearing leg and the healthy leg expressed as % referred to the control animals. CDDP = cisplatin.

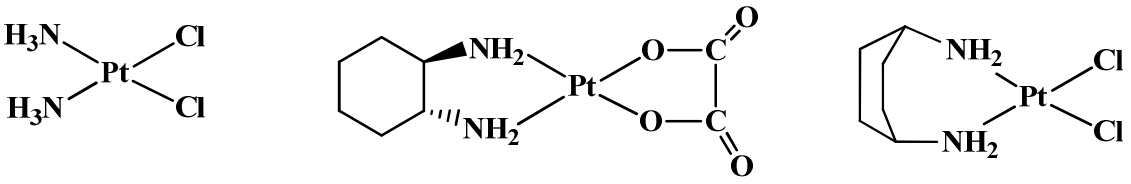

Cisplatin **Oxaliplatin** **Kiteplatin**

Figure 1. Pt(II) complexes.

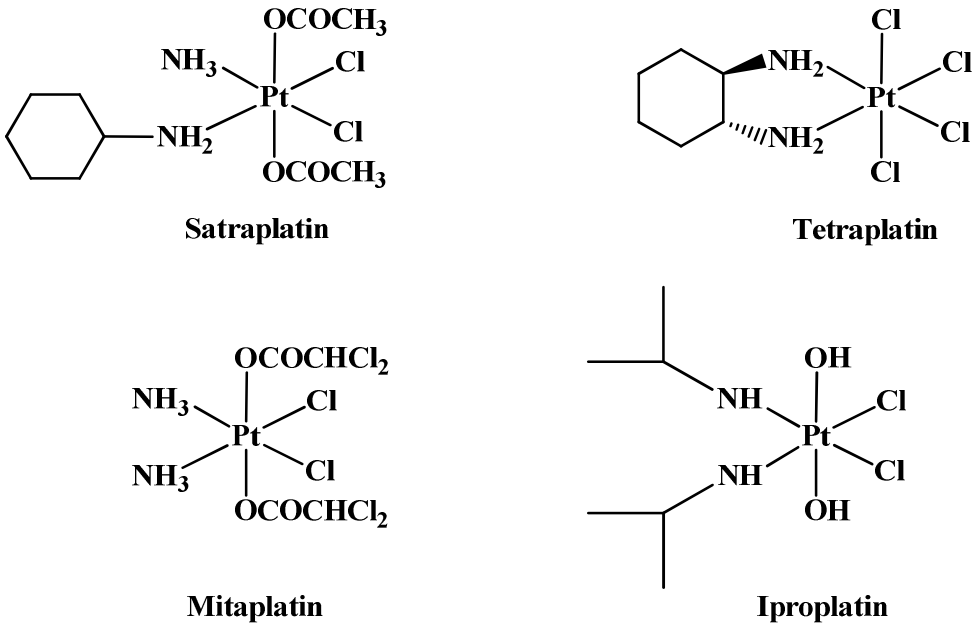

Figure 2. Pt(IV) complexes.

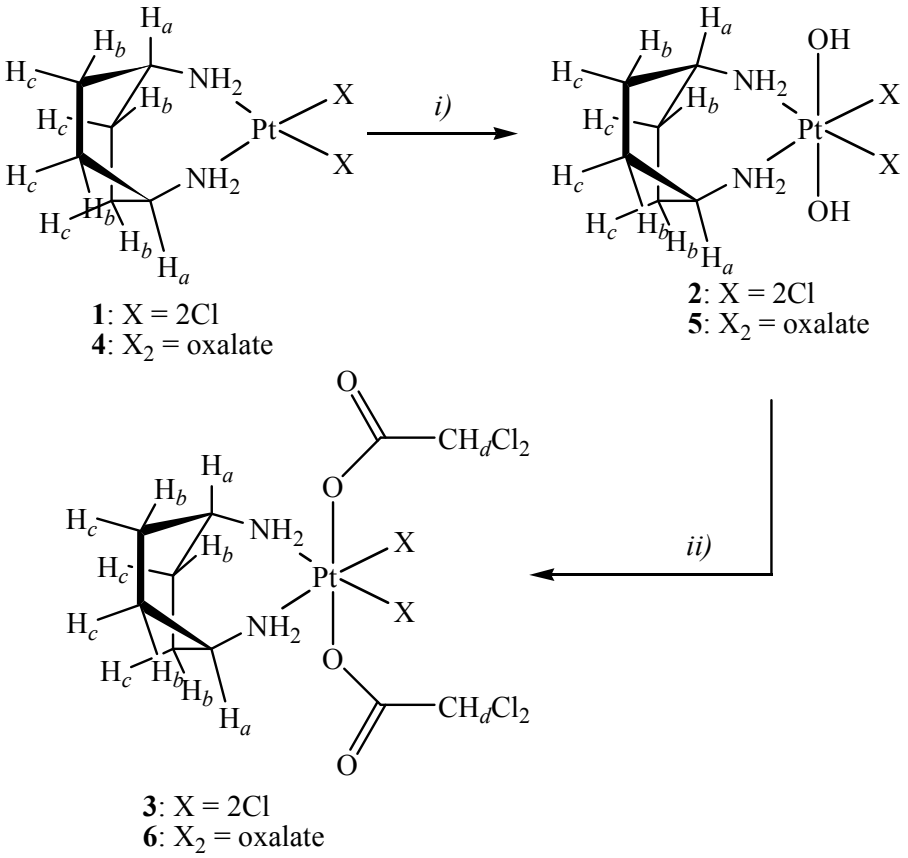

Scheme 1. Synthesis of complexes **2-6**. *i*) H_2O, exc. H_2O_2, 70 °C, dark, 2h. *ii*) THF, exc. DCA, r.t., dark, 17 h.

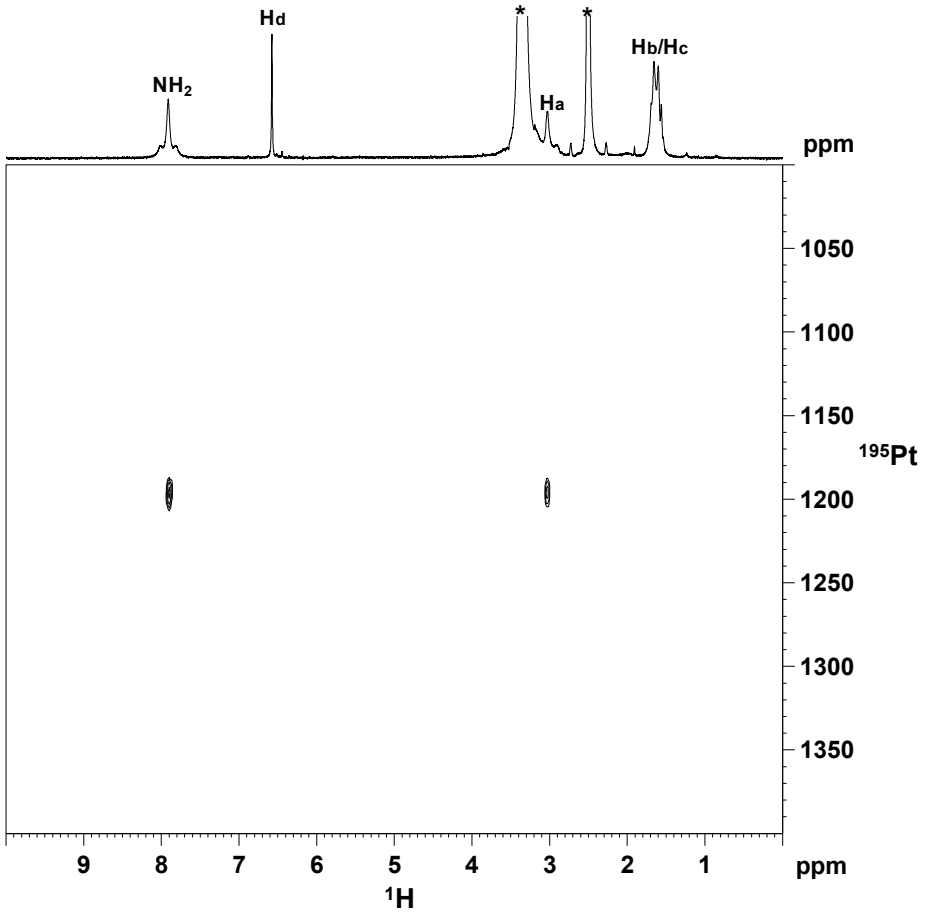

Figure 3. ^{1}H (top) and [^{1}H-^{195}Pt] HSQC 2D (bottom) NMR (300 MHz, ^{1}H) spectra of **3** in DMSO-d_6, the asterisks indicate residual solvent peaks.

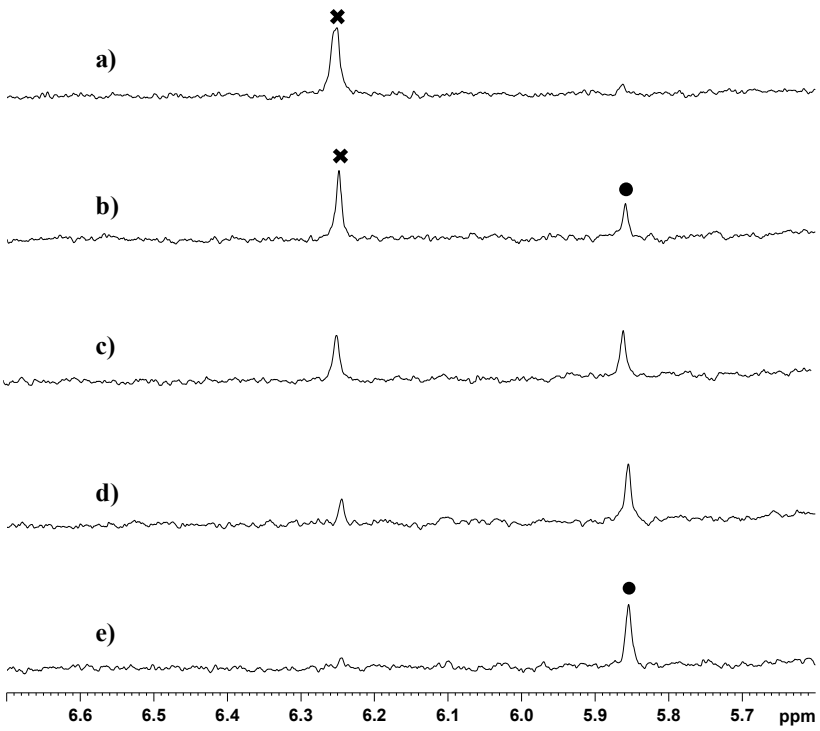

Figure 4. Portion of the ^{1}H-NMR (300 MHz, ^{1}H) spectra of compound **3** in deuterated aqueous, phosphate buffered, saline solution (7.87 mM, pH 7.4; 10% V/V DMSO-d_6), recorded at zero time (a), 30 min (b), 1 hour (c), 2 hours (d), and 3 hours (e) at 37 °C. ✖ indicates the peak of coordinated DCA in complex **3**. ● indicates the peak of free DCA.

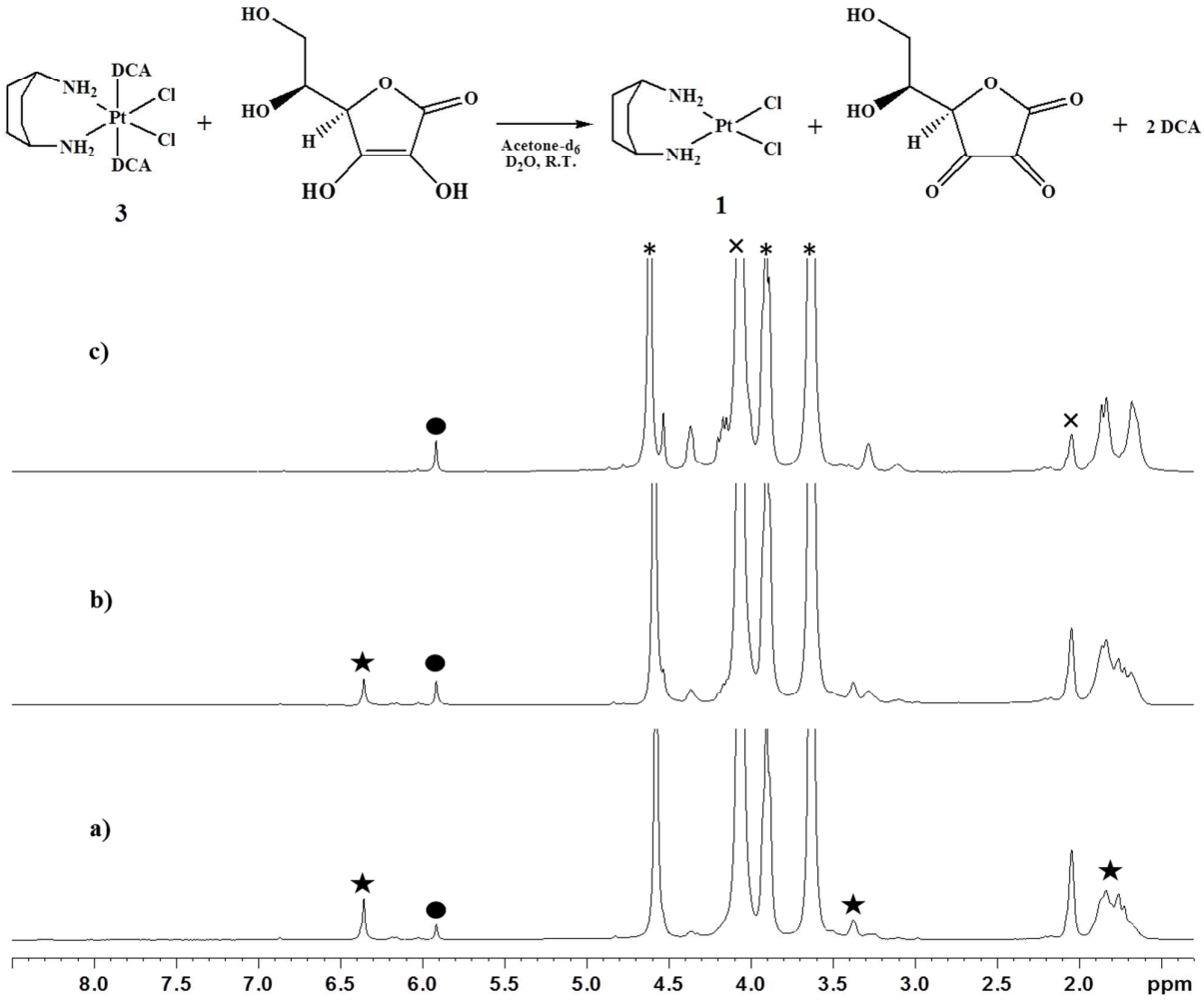

Figure 5: ^{1}H NMR spectra of compound **3** treated with an excess (1:5 molar ratio) of a 1:1 mixture of ascorbic acid/sodium ascorbate in Acetone-d_6/D_2O (550/100, v/v) at zero time (a) and after 20 minutes at 25 °C (b) and 45 minutes at 37 °C (c). The asterisks indicate the peaks belonging to the excess of ascorbic acid/ascorbate present in solution. The two × indicate residual solvent peaks. The stars indicate the peaks of starting complex **3**. ● indicates the peak of free DCA. The new species showing peaks in the region 4.0-4.5 ppm (spectrum c) most likely corresponds to the hydrated bicyclic form of ascorbic acid.

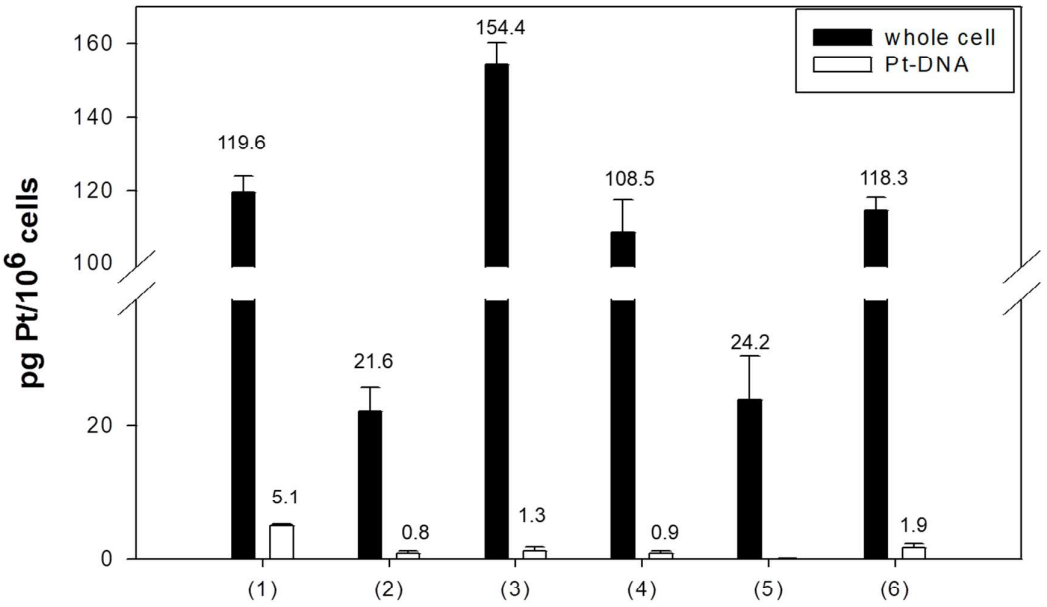

Figure 6. Intracellular accumulation and DNA-platination induced by compounds **1-6**. BxPC3 cells were incubated with 5 μM concentration of tested compound for 24 h. The Pt cellular content was estimated by means of GF-AAS analysis. Data are the means of three independent experiments. Error bars indicate S.D.

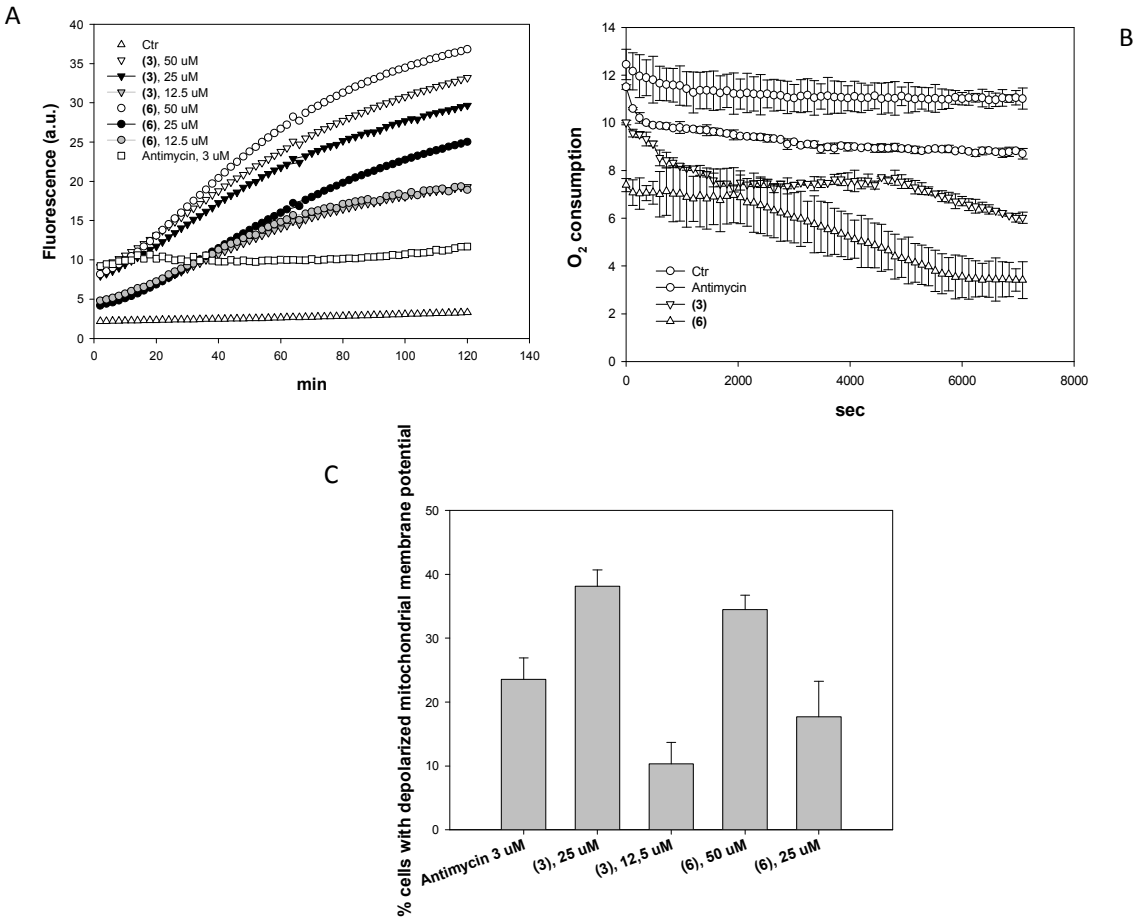

Figure 7. Effects induced by compounds **3** and **6** at mitochondrial level. **A.** ROS production in BxPC3 cells. Cells were pre-incubated in PBS/10 mM glucose medium for 20 min at 37 °C in the presence of 10 mM CM-H_2DCFDA and then treated with increasing concentrations of **3**, **6** or Antimycin (3 μM). Fluorescence of DCF was measured at 485 nm (excitation) and 527 nm (emission). **B.** Effects of derivatives **3** and **6** on O_2 consumption. BxPC3 cells were treated with Mito-ID® O_2 Sensor Probe Solution containing IC_{50} of tested compounds. Fluorescence was estimated at 350 nm (excitation) and 610 nm (emission). Data are the means of five independent experiments. **C.** Effects of **3** and **6** on mitochondrial membrane potential. BxPC3 cells were treated for 24 h with increasing concentrations of **3**, **6** or Antimycin (3 μM) and stained with TMRM (10 nM). Fluorescence was estimated at 490 nm (excitation) and 590 nm (emission). Data are the means of five independent experiments. Error bars indicate S.D.

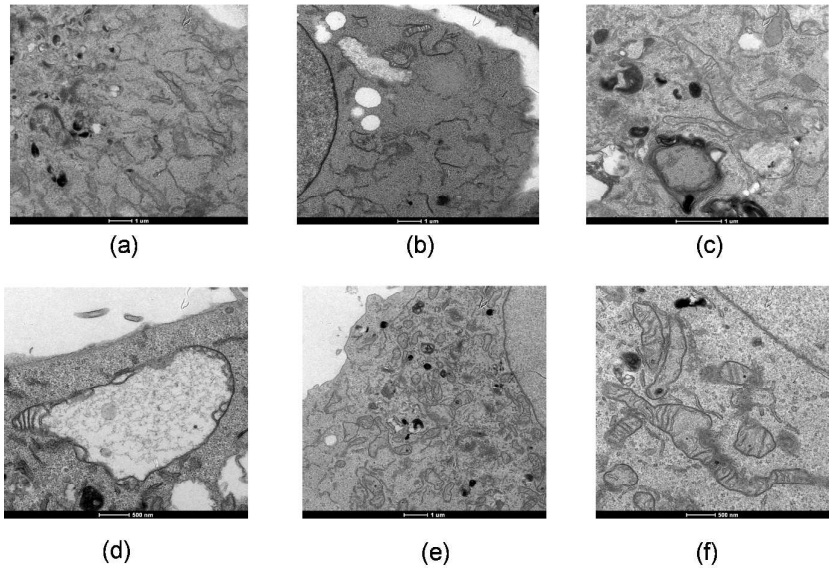

Figure 8. TEM analysis of BxPC3 cells treated for 12 or 24 h with IC_{50} of **3** and **6**. Cells were processed through standard procedures as reported in the Experimental Section. a) and b) Control; c) **3**, 12 h; d) **3**, 24 h; e) **6**, 12 h; f) **6**, 24 h.

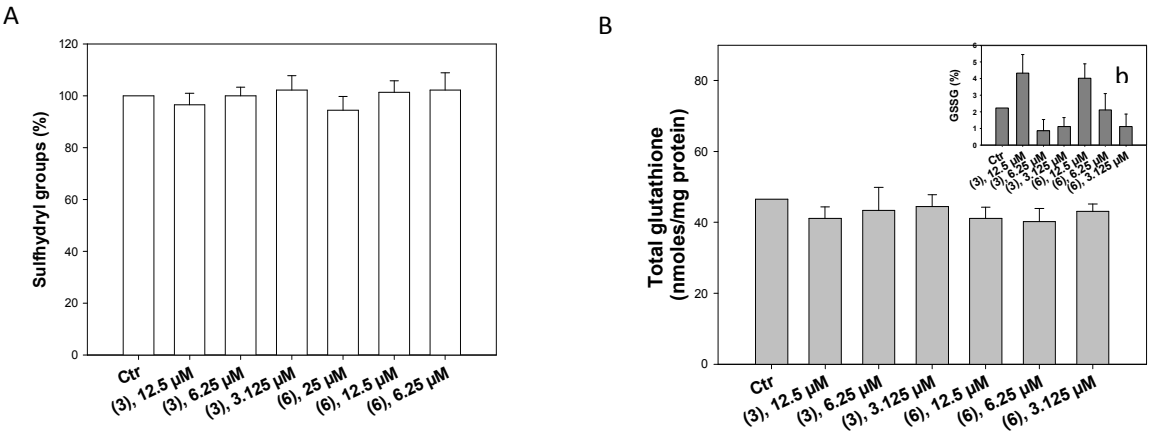

Figure 9. Effect of compounds **3** and **6** on the redox cellular environment. BxPC3 cells were treated for 48 h with increasing concentrations of **3** and **6**. The amount of sulfhydryl group (**A**), total glutathione (GSH+GSSG, **B**) and oxidized glutathione (**B**, inset b) were measured by means of DTNB reaction as reported in the Experimental Section.

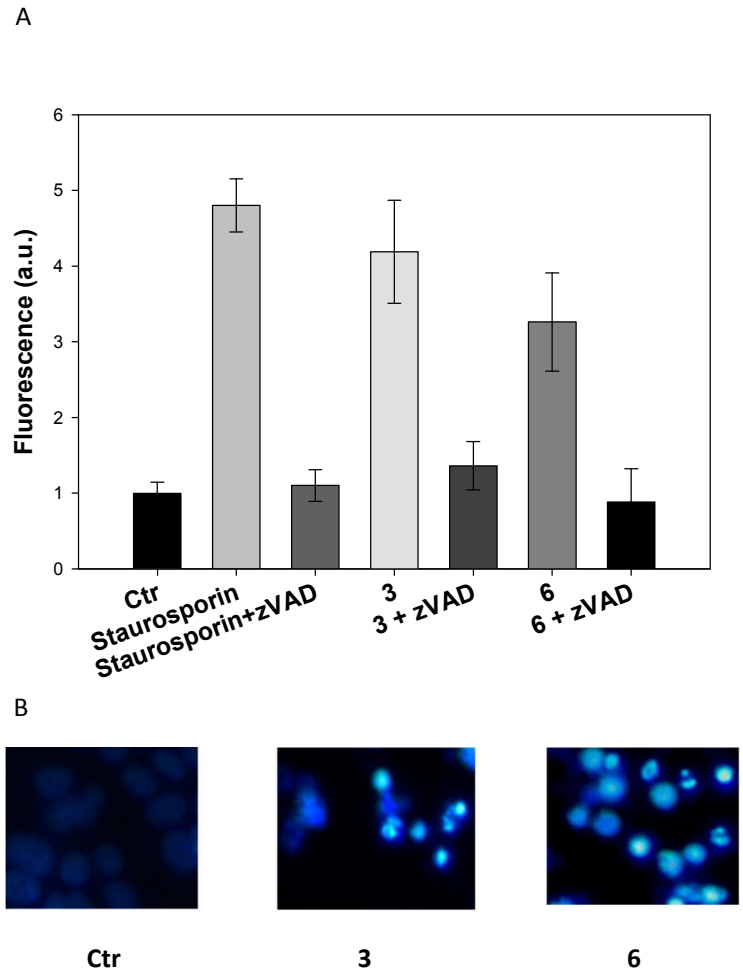

Figure 10. Induction of apoptosis. **A.** Caspase activity: BxPC3 cells were incubated for 24 h with increasing concentration of **3** and **6** or staurosporine ± broad-spectrum caspase inhibitor zVAD, and processed for caspase-3/7 activity. Data are the means of three independent experiments. Error bars indicate S.D. **B.** Apoptotic bodies formation: BxPC3 cells were treated with IC_{50} of **3** for 48 h and stained with the fluorescent dye Hoechst 33258.

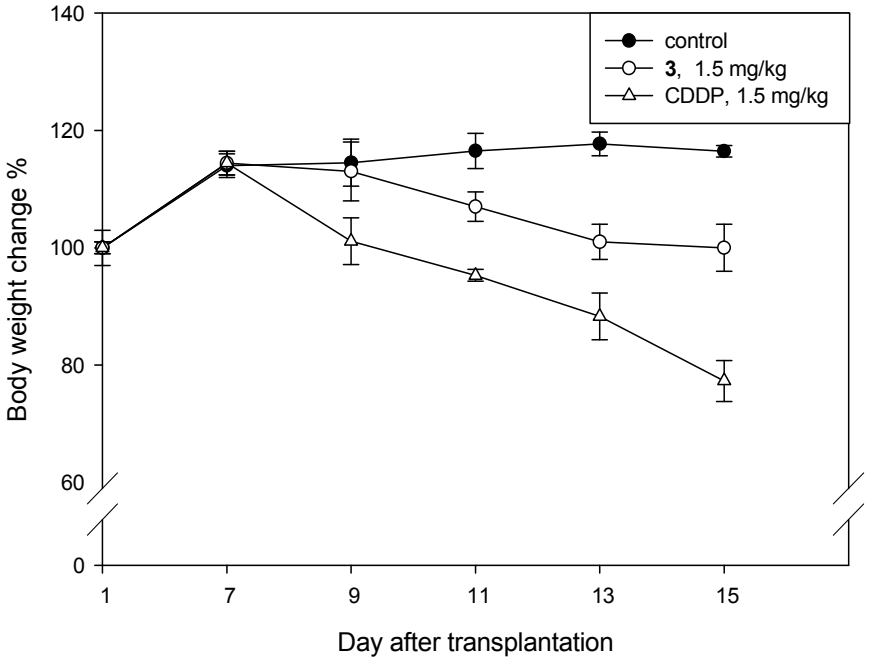

Figure 11. Body weight changes. The body weight changes of LLC bearing C57BL mice treated with vehicle or tested compounds. Each drug was administered daily after 7 days from the tumor cell inoculum. Weights were measured at day 1 and daily from day 7. Error bars indicate S.D.. CDDP = cisplatin.

Table of contents entry

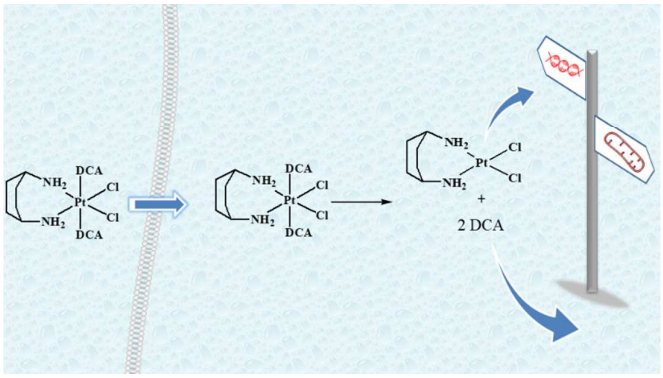

DNA and mitochondria of tumor cells are the targets of Pt(IV) complexes of kiteplatin with biologically active dichloroacetate as axial ligands.

References

[1] B. Lippert, Ed. *Cisplatin: Chemistry and Biochemistry of a Leading Anticancer Drug*; Verlag Helvetica Chimica Acta: Zürich, 1999; pp. 563.

[2] B. Rosenberg, L. VanCamp, J. E. Trosko, V. H. Mansour. Platinum compounds: a new class of potent antitumour agents. *Nature*. 1969, **222**, 385-386.

[3] D. Wang, S. J. Lippard. Cellular processing of platinum anticancer drugs. *Nat. Rev. Drug Discovery*. 2005, **4**, 307-320.

[4] P.M. Bruno, Y. Liu, G.Y. Park, J. Murai, C.E. Koch, T.J. Eisen, J.R. Pritchard, Y. Pommier, S.J. Lippard, M. T. Hemann. A subset of platinum-containing chemotherapeutic agents kills cells by inducing ribosome biogenesis stress. *Nat. Med.* 2017, **23**, 461-473.

[5] M. Galanski, M.A. Jakupec, B.K. Keppler. Update of the preclinical situation of anticancer platinum complexes: Novel design strategies and innovative analytical approaches. *Curr. Med. Chem.* 2005, **12**, 2075-2094.

[6] B. Rosenberg, L. VanCamp, T. Krigas. Inhibition of Cell Division in *Escherichia coli* by Electrolysis Products from a Platinum Electrode. *Nature*. 1965, **205**, 698-699.

[7] Y. Shi, S.-A. Liu, D.J. Kerwood, J. Goodisman, J.C. Dabrowiak. Pt(IV) complexes as prodrugs for cisplatin. *J. Inorg. Biochem*. 2012, **107**, 6-14.

[8] M.D. Hall, R.C. Dolman, T.W. Hambley. *Metal ions in biological systems* (*Metal Complexes in Tumor Diagnosis and as Anticancer Agents*); Sigel, A.; Sigel, H., Eds.; Dekker M., Inc.: New York, 2004; **vol 42**, pp. 298-322.

[9] M. D. Hall, T.W. Hambley. Platinum(IV) antitumour compounds: their bioinorganic chemistry. *Coord. Chem. Rev*. 2002, **232**, 49-67.

[10] M.D. Hall, R.A. Alderden, M. Zhang, P.J. Beale, Z. Cai, B. Lai, A.P.J. Stamp, T.W. Hambley. The fate of platinum(II) and platinum(IV) anti-cancer agents in cancer cells and tumours. *J. Struct. Biol*. 2006, **155**, 38-44.

[11] M.D. Hall, H.R. Mellor, R. Callaghan, T.W. Hambley. Basis for design and development of platinum(IV) anticancer complexes. *J. Med. Chem*. 2007, **50,** 3403-3411.

[12] A.M. Montana, C. Batalla. The rational design of anticancer platinum complexes: the importance of the structure-activity relationship. *Curr. Med. Chem*. 2009, **16**, 2235-2260.

[13] J.J. Wilson, S.J. Lippard. Synthesis, characterization, and cytotoxicity of platinum(IV) carbamate complexes. *Inorg*. *Chem*. 2011, **50**, 3103-3115.

[14] P. Gramatica, E. Papa, M. Luini, E. Monti, M.B. Gariboldi, M. Ravera, E. Gabano, L. Gaviglio. D. Osella. Antiproliferative Pt(IV) complexes: synthesis, biological activity, and quantitative structure-activity relationship modeling. *J. Biol*. *Inorg*. *Chem*. 2010, **15**, 1157-1169.

[15] T.C. Johnstone, K. Suntharalingam, S.J. Lippard. The Next Generation of Platinum Drugs: Targeted Pt(II) Agents, Nanoparticle Delivery, and Pt(IV) Prodrugs. *Chem. Rev.* 2016, **116**, 3436−3486.

[16] M.R. Reithofer, M. Galanski, A. Roller, B.K. Keppler. An Entry to Novel Platinum Complexes: Carboxylation of Dihydroxoplatinum(IV) Complexes with Succinic Anhydride and Subsequent Derivatization. *Eur. J. Inorg*. *Chem*. 2006, 2612-2617.

[17] S. Theimer, H.P. Varbanov, M. Galanski, A.E. Egger, W. Berger, P. Heffeter, B.K. Keppler. Comparative in vitro and in vivo pharmacological investigation of platinum(IV) complexes as novel anticancer drug candidates for oral application. *J. Biol. Inorg. Chem*. 2015, **20**, 89-99.

[18] K.R. Barnes, A. Kutikov, S.J. Lippard. Synthesis, characterization, and cytotoxicity of a series of estrogen-tethered platinum(IV) complexes. *Chem. Biol.* 2004, **11**, 557-564.

[19] S. Dhar, S.J. Lippard. Mitaplatin, a potent fusion of cisplatin and the orphan drug dichloroacetate. *PNAS*. 2009, **106**, 22199-22204.

[20] O. Warburg. On the origin of cancer cells. *Science*. 1956, **123**, 309-314.

[21] S. Fulda, L. Galluzzi, G. Kroemer. Targeting mitochondria for cancer therapy. *Nature Rev., Drug Discovery*. 2010, **9**, 447-464.

[22] P.W. Stacpoole, N.V. Nagaraja, A.D. Hutson. Efficacy of dichloroacetate as a lactate-lowering drug. *J. Clin. Pharmacol*. 2003, **43**, 683-691.

[23] S. Kankotia, P.W. Stacpoole. Dichloroacetate and cancer: new home for an orphan drug? *Biochim. Biophys. Acta*. 2014, 1846, 617-629.

[24] E.D. Michelakis, L. Webster, J.R. Mackey. Dichloroacetate (DCA) as a potential metabolic-targeting therapy for cancer. *Br. J. Canc*. 2008, **99**, 989-994.

[25] N. Margiotta, C. Marzano, V. Gandin, D. Osella, M. Ravera, E. Gabano, J.A. Platts, E. Petruzzella, J.D. Hoeschele, G. Natile. Revisiting [$PtCl_2$(*cis*-1,4-DACH)]: an underestimated antitumor drug with potential application to the treatment of oxaliplatin-refractory colorectal cancer. *J. Med. Chem*. 2012, **55**, 7182-7192.

[26] J. Kasparkova, T. Suchankova, A. Halamikova, L. Zerzankova, O. Vrana, N. Margiotta, G. Natile, V. Brabec. Cytotoxicity, cellular uptake, glutathione and DNA interactions of an antitumor large-ring Pt(II) chelate complex incorporating the *cis*-1,4-diaminocyclohexane carrier ligand. *Biochem. Pharmacol*. 2010, **79**, 552−564.

[27] V. Brabec, J. Malina, N. Margiotta, G. Natile, J. Kasparkova. Thermodynamic and mechanistic insights into translesion DNA synthesis catalyzed by Y-family DNA polymerase

across a bulky double-base lesion of an antitumor platinum drug. *Chem. Eur. J.* 2012, **18**, 15439-15448.

[28] S. Shamsuddin, I. Takahashi, Z.H. Siddik, A.R. Khokhar. Synthesis, characterization, and antitumor activity of a series of novel cisplatin analogs with cis-1,4-diaminocyclohexane as nonleaving amine group. *J. Inorg. Biochem*. 1996*,* **61***,* 291-301.

[29] M.R. Reithofer, S.M. Valiahdi, M.A. Jakupec, V.B. Arion, A. Egger, M. Galanski, B.K. Keppler. Novel di- and tetracarboxylatoplatinum(IV) complexes. Synthesis, characterization, cytotoxic activity, and DNA platination. *J. Med. Chem.* 2007, **50**, 6692-6699.

[30] E. Petruzzella, N. Margiotta, M. Ravera, G. Natile. NMR investigation of the spontaneous thermal- and/or photoinduced reduction of trans dihydroxido Pt(IV) derivatives. *Inorg. Chem*. 2013, **52**, 2393-2403.

[31] W.H. Ang, S. Pilet, R. Scopelliti, F. Bussy, L. Juillerat-Jeanneret, P.J. Dyson. Synthesis and characterization of platinum(IV) anticancer drugs with functionalized aromatic carboxylate ligands: influence of the ligands on drug efficacies and uptake. *J. Med. Chem*. 2005, **48**, 8060-8069.

[32] E. Wexselblatt, E. Yavin, D. Gibson. Platinum(IV) prodrugs with haloacetato ligands in the axial positions can undergo hydrolysis under biologically relevant conditions. *Angew. Chem. Int. Ed*. 2013, **52**, 6059-6062.

[33] V. Pichler, P. Heffeter, S.M. Valiahdi, C.R. Kowol, A. Egger, W. Berger, M.A. Jakupec, M. Galanski, B.K. Keppler. Unsymmetric mono- and dinuclear platinum(IV) complexes featuring an ethylene glycol moiety: synthesis, characterization, and biological activity. *J. Med. Chem.* 2012, **55**, 11052-11061.

[34] C.F. Chin, D.Y.Q. Wong, R. Jothibasu, W.H. Ang. Anticancer platinum (IV) prodrugs with novel modes of activity. *Curr. Trends Med. Chem.* 2011, **11**, 2602–2612.

[35] E. Wexselblatt, D. Gibson. What do we know about the reduction of Pt(IV) pro-drugs? *J. Inorg. Biochem.* 2012, **117**, 220–229.

[36] J. Zajac, H. Kostrhunova, V. Novohradsky, O. Vrana, R. Raveendran, D. Gibson, J. Kasparkova, V. Brabec. Potentiation of mitochondrial dysfunction in tumor cells by conjugates with a Pt(IV) derivative of oxaliplatin. *J. Inorg. Biochem.* 2016, **156**, 89-97.

[37] A.R. Khokhar, S. Al-Baker, S. Shamsuddin, Z.H. Siddik. Chemical and biological studies on a series of novel (trans-(1R,2R)-, trans-(1S,2S)-, and cis-1,2-diaminocyclohexane)platinum(IV) carboxylate complexes. *J. Med. Chem.* 1997, **40**, 112–116.

[38] E. Wexselblatt, R. Raveendran, S. Salameh, A. Friedman-Ezra, E. Yavin, D. Gibson. On the stability of Pt(IV) Pro-Drugs with Haloacetato Ligands in the Axial Positions. *Chem. Eur. J.* 2015, **21**, 3108-3114.

[39] L. Cubo, T.W. Hambley, P.J.S. Miguel, A. Carnero, C, Navarro-Ranninger, A.G. Quiroga, The preparation and characterization of trans-platinum(IV) complexes with unusually high cytotoxicity. *Dalton Trans.* 2011, **40**, 344-347.

[40] R.K. Pathak, S. Marrache, D.A. Harn, S. Dhar. Mito-DCA: a mitochondria targeted molecular scaffold for efficacious delivery of metabolic modulator dichloroacetate. *ACS Chem. Biol*. 2014, **9**, 1178-1187.

[41] G. Marverti, P.A. Andrews, G. Piccinini, S. Ghiaroni, D. Barbieri, M.S. Moruzzi. Modulation of cis-diamminedichloroplatinum (II) accumulation and cytotoxicity by spermine in sensitive and resistant human ovarian carcinoma cells. *Eur J. Cancer*. 1997, **33**, 669-675.

[42] P.A. Andrews, M.P. Murphy, S.B. Howell. Differential potentiation of alkylating and platinating agent cytotoxicity in human ovarian carcinoma cells by glutathione depletion. *Cancer Res*. 1985, **45**, 6250-6253.

[43] K.J. Scanlon, M. Kashani-Sabet, T. Tone, T. Funato. Cisplatin resistance in human cancers. *Pharmacol. Ther*. 1991, **52**, 385–406.

[44] C. Marzano, V. Gandin, A. Folda, G. Scutari, A. Bindoli, M.P. Rigobello. Inhibition of thioredoxin reductase by auranofin induces apoptosis in cisplatin-resistant human ovarian cancer cells. *Free Radic. Biol. Med.* 2007, **42**, 872–881.

[45] L. Ekblad, J. Kjellström, A. Johnsson. Reduced drug accumulation is more important in acquired resistance against oxaliplatin than against cisplatin in isogenic colon cancer cells. *Anticancer Drugs*. 2010, **21**, 523-531.

[46] D. Theile, S. Grebhardt, W.E. Haefeli, J. Weiss. Involvement of drug transporters in the synergistic action of FOLFOX combination chemotherapy. *Biochem. Pharmacol.* 2009, **78**, 1366-1373.

[47] J.D. Page, I. Husain, A. Sancar, S.G. Chaney. Effect of the diaminocyclohexane carrier ligand on platinum adduct formation, repair, and lethality. *Biochemistry*. 1990, **29**, 1016−1024.

[48] D. Trachootham, W. Lu, M.A. Ogasawara, R.D. Nilsa, P. Huang. Redox regulation of cell survival. *Antioxid. Redox Signal.* 2008, **10**, 1343-1374.

[49] M.L. Circu, T.Y. Aw. Glutathione and apoptosis. *Free Radic. Res*. 2008, **42**, 689–706.

[50] S. Temraz, D. Mukherji, R. Alameddine, A. Shamseddine. Methods of overcoming treatment resistance in colorectal cancer. *Crit. Rev. Oncol. Hematol*. 2014, **89**, 217-230.

[51] D.S. Wishart, C.G. Bigam, J. Yao, F. Abildgaard, H.J. Dyson, E. Oldfield, J.L. Markley, B.D. Sykes. ^{1}H, ^{13}C and ^{15}N chemical shift referencing in biomolecular NMR. *J. Biomolecular NMR*. 1995, **6**, 135-140.

[52] P.S. Pregosin. Platinum-195 nuclear magnetic resonance. *Coord. Chem. Rev.* 1982, **44**, 247-291.

[53] R. Ranaldo, N. Margiotta, F.P. Intini, C. Pacifico, G. Natile. Conformer distribution in (cis-1,4-DACH)bis(guanosine-5'-phosphate)platinum(II) adducts: a reliable model for DNA adducts of antitumoral cisplatin. *Inorg. Chem*. 2008, **47**, 2820-2830.

[54] V. Gandin, M. Pellei, F. Tisato, M. Porchia, C. Santini, C. Marzano. A novel copper complex induces paraptosis in colon cancer cells via the activation of ER stress signalling. *J. Cell. Mol. Med.* 2012, **16**, 142-151.

[55] M. P. Rigobello, V. Gandin, A. Folda, A.-K. Rundloef, A.P. Fernandes, A. Bindoli, C. Marzano, M. Bjoernstedt. Treatment of human cancer cells with selenite or tellurite in combination with auranofin enhances cell death due to redox shift. *Free Radic. Biol. Med.* 2009, **47**, 710–721.

[56] A. Bindoli, M.T. Callegaro, E. Barzon, M. Benetti, M.P. Rigobello. Influence of the redox state of pyridine nucleotides on mitochondrial sulfhydryl groups and permeability transition. *Arch. Biochem. Biophys*. 1997, **342**, 22–28.